A NUMERICAL STUDY OF THE EFFECTS OF THE ROUGHNESS LENGTH ON THE MESO-SCALE FLOW PATTERNS OVER KENYA.

BY

MATAYO INDEJE

A thesis submitted in part fulfilment for the degree of Master of Science in the Department of Meteorology at the University of Nairobi, Kenya.

October 1992.

DECLARATION

This thesis is my original work and has not been presented for a degree in any other University

Signature

Dat. . . . . &tl?J.%h.

This thesis has been submitted for examination with our approval as University supervisors.

Prof. L,J. Ogallo

Date ....

Dr. E.K. Anyamba

Signature ..

Date .. fc

Department of Meteorology

University of Nairobi

P.O. BOX 30297

NAIROBI

KENYA.

TABLE OF CONTENTS **PAGE**

LIST OF FIGURES (Contd.)

LIST OF FIGURES (Contd.)

ABSTRACT.

A three-dimensional numerical model was used in this study to examine the effects of changes in the surface roughness length on the meso-scale flow patterns over Kenya.

Three experiments were performed. The first experiment was performed to test the ability of the model in reproducing the meso-scale circulations over Kenya. In the second experiment, the roughness length was uniform over the whole domain (homogeneous roughness terrain). Three values of the surface roughness were used in this experiment, namely 15cm, 110cm, and 10cm to represent the Savannah grasslands, Urban conditions and Desert conditions respectively. In the third experiment, the roughness length at each grid point was specified according to the terrain characteristics (heterogeneous roughness terrain). The initial fields were observations for May 6 1986.

Results of the first experiment showed that the model was able to give realistic simulations of the meso-scale flow over Kenya. The model simulated the afternoon sea/lake breezes and upslope flows on either side of the Kenya highlands. In the morning, the land breeze and downslope flows from the Kenya highlands were also simulated. Maximum afternoon low-level rising motion, meso-scale convergence and precipitation were located over the western highlands.

Results from the second experiment showed that changes in the surface roughness had significant impacts on the development of meso-scale flows over Kenya. The simulated boundary layer wind speed decreased as the surface roughness was increased. The results further showed enhanced turbulent mixing of the boundary layer heat and moisture, and increased convective rainfall over the western highlands, when the surface roughness was increased. Non-convective rainfall contributed relatively less to the total simulated meso-scale rainfall over Kenya.

In the third experiment, it was found that the simulated boundary layer wind field compared well with the mean flow patterns for May. The simulated temperature field indicated high values over the coastal areas, the lake region and the arid and semi-arid northern parts of Kenya. Low temperatures were concentrated over the central highlands. These patterns compared well with the observed mean patterns for the month. High values of relative humidity were simulated over the coastal areas and western highlands in agreement with the observations. Rising motion accompanied by high meso-scale precipitation was simulated over western Kenya, while the eastern highlands including the arid/semi arid areas of northern Kenya were dry. These results compared better with the mean fields and the observed weather patterns for May 6 1986.

From the results obtained in this study one may infer that modification of the land surface characteristics through human activities like deforestation and overgrazing, would have considerable impacts on the meso-scale weather systems in Kenya. Such changes would have far reaching socio-economic impacts. Proper planning of land use activities is therefore recommended in order to minimize human induced modification of the surface characteristics.

Finally, the results form a first step towards the parameterization of the surface characteristics in meso-scale numerical studies in Kenya.

LIST OF FIGURES

LIST OF FIGURES (Contd.)

LIST OF FIGURES (Contd.)

LIST OF FIGURES (Contd.)

LIST OF TABLES

DEFINITION OF SYMBOLS AND PHYSICAL CONSTANTS

b	Fraction of total water-vapour convergence used to moisten grid column in cumulus parameterization scheme.
C_p	Specific heat at constant pressure for dry air.
$C_{p,,}$	Specific heat at constant pressure for moist air.
C*	Condensation and evaporation rates.
C_g	Thermal capacity of slab per unit area.
E,	Flux of water vapour from surface into atmosphere.
f	Coriolis parameter.
$F_{h,,}$	Term representing contribution of horizontal diffusion of a variable a to the temporal rate of change of a.
F_{Va}	Term representing contribution of vertical diffusion of a variable a to the temporal rate of change of a.
g	Acceleration due to gravity.
h	Height of the planetary boundary layer.
H_m	Heat flux into the substrate.
H,	Sensible-heat flux from the surface into the atmosphere.
I	Function of static stability and surface friction velocity, used to compute latent heat flux from the surface.
K,	Background molecular diffusivity.
K_h	Horizontal eddy diffusion.
K_m	Coefficient of heat transfer from the ground into the substrate.
K_z	Coefficient of vertical diffusivity (m^2 s^{-1}) .
K^,	Background value of K_z (egual to 1.0 m^2 s^{-1}) .
L	Monin-Obukhov length.

L_v	Latent heat of condensation.
l	Vertical mixing length,
m	Map scale factor.
M	Surface moisture availability.
M_c	Critical value of moisture convergence (3.0×10^5 $Kgm^{-2}s^{-1}$) .
M_v	Vertical integral of horizontal convergence of water vapour.
N_h	Nondimensional function for the vertical profile of convective heating.
N_m	Nondimensional function for the vertical profile of convective moistening.
P	Pressure.
P_0	Reference pressure.
P_s	Surface pressure.
P_t	Pressure at the top of the model.
P*	$P_s - P_t$.
q_c	Mixing ratio of cloud water.
q_r	Mixing ratio of rain water.
q_v	Mixing ratio of water vapour.
q_c	Mixing ratio of water vapour in cumulus cloud.
q_s	Saturation mixing ratio of water vapour.
Q	Diabatic heating rate per unit mass.
Q_s	Net short-wave irradiance at the surface.
R	Ideal gas constant for dry air.
RH	Relative humidity.
R_n	Net radiation.

R_{jb}	Bulk Richardson number.
R_{jc}	Critical value of Richardson number.
t	Time.
T	Temperature.
T_g	Temperature of ground.
T_v	Virtual temperature.
T.	Surface "friction" temperature.
u	Component of wind velocity in eastward direction,
u.	Surface frictional velocity.
v	Component of wind velocity in northward direction.
V	Horizontal wind vector.
V,	Horizontal wind speed at lowest model layer.
V_c	Convective PBL velocity.
V^	Divergence of the vertical eddy flux of water vapour due to convective clouds.
w_p	Precipitable water.
x	Horizontal grid coordinate increasing eastwards,
y	Horizontal grid coordinate increasing northwards,
z	Height above the surface,
z.	Height of the lowest layer in model.
$z_{„}$	Surface roughness length.
	Background value of z_0 over water (10"* m) .
z,	Depth of the molecular layer,
a	Symbol representing any prognostic variable.
X	Thermal inertia.
Ax,Ay	Horizontal grid size in x and y directions respectively.

Aa	Thickness of the model a-layers.
At	Time step.
Az	Thickness of the vertical layer.
6	Entrainment coefficient used in high resolution PBL model.
e,	Atmospheric emissivity.
e_f	Emissivity of the ground (slab).
d	Potential temperature, and also latitude.
$0v_t$	Potential temperature at the lowest layer in model.
$0v_g$	Potential temperature of the ground surface.
0_U	Virtual potential temperature.
X	Thermal conductivity.
K	Von KSrman constant,
p.	Density of air.
$\dot{a}$	Nondimensional vertical coordinate of the model.
a	Vertical velocity in a-coordinates.
r	Surface stress.
$<p$	Geopotential.
$\backslash p_m$	Nondimensional stability parameter for momentum.
$\backslash p_h$	Nondimensional stability parameter for heat and water vapour.
OJ	Vertical velocity in pressure coordinates,
n	Angular velocity of the earth.

CHAPTER 1

1.0 INTRODUCTION

The surface roughness length or parameter (z_o), is a measure of the resistance to the airflow caused by the underlying physical characteristics of different surfaces. The roughness length of a place depends on the vegetation cover (forests, grasslands, etc.), geomorphological factors (mountains, hills, valleys), and man-made structures such as high-rise buildings in urban areas.

The roughness length is lowest over the smooth surfaces of desert areas and increases with the increase in the obstruction the airflow encounters as it passes over grasslands, forests, mountains and urban areas. The roughness length is defined mathematically by the wind profile eguation in the lowest part of the planetary boundary layer (PBL), where the velocity profile is adjusted so that the horizontal frictional stress is independent of height. The turbulent mixing in this layer is due to dynamic instability as a result of strong vertical wind shear near the ground (i.e this lowest layer is mechanically driven, not thermally driven).

The simplified wind profile equation in this layer is given as:

$$u = \frac{}{K} \ln\left(\frac{}{Z_N}\right)$$

where

u* is the frictional velocity

K is Von-KSrmSn constant

z is the height of the resisting surface, and

z_Q is the roughness length

This equation applies only during neutral stability conditions.

As air flows over the resisting surfaces with different roughness lengths, the transfer of mass, momentum and heat between the land surface and the atmosphere is considerably modified. The interaction between land and atmosphere play an important role in the climate system (i.e land, ocean, cryosphere, and atmosphere) . Specifically, the fluxes of radiation, momentum and sensible heat between the atmosphere and the underlying surface influence the atmospheric motion, temperature, humidity and precipitation fields which in turn feed back onto the spatial distribution of sinks and sources of these fluxes on the land surface. The three land surface properties which ultimately govern this interactions are albedo, surface roughness and surface hydrological characteristics. These properties influence radiative transfer, momentum transfer and sensible and latent heat transfer, respectively between the atmosphere and the underlying surfaces (Sud and Smith 1985a).

Sensitivity studies have been used as one of the methods

of examining the impacts of changes in albedo, surface roughness and perhaps more importantly, the surface wetness to the atmospheric fields. The planetary boundary layer is a region of variable depth which frequently acts as a buffer zone where heat, moisture, momentum and pollution fed into it (or extracted from it) from the underlying surface are stored and accumulated until such a time that for one or various reasons, the boundary layer 'breaks down'. The contents within the PBL are hence redistributed through a much greater depth of the atmosphere, where it can affect synoptic changes on totally different scales than hitherto (Sud et al. 1988) . The surface roughness has been found to control the diurnal evolution of the PBL, which is a critical factor in producing meso-scale weather systems such as convective storms, land-sea breezes, thermal boundaries, and mountain-valley circulations (Zhang and Anthes 1982). The surface roughness also influences precipitation due to its direct effect on the boundary layer water vapour transport and convergence.

Observational studies by Asnani and Kinuthia (1979), and numerical studies by Okeyo (1982, 1987), have shown that meso-scale systems play an important role in determining the diurnal wind and rainfall patterns over Kenya. The main aim of this study is to examine the impacts of changing the roughness length on the development of meso-scale flow over Kenya. The domain of study is bounded by 5°N and 5°S, and 33°E and 43°E.

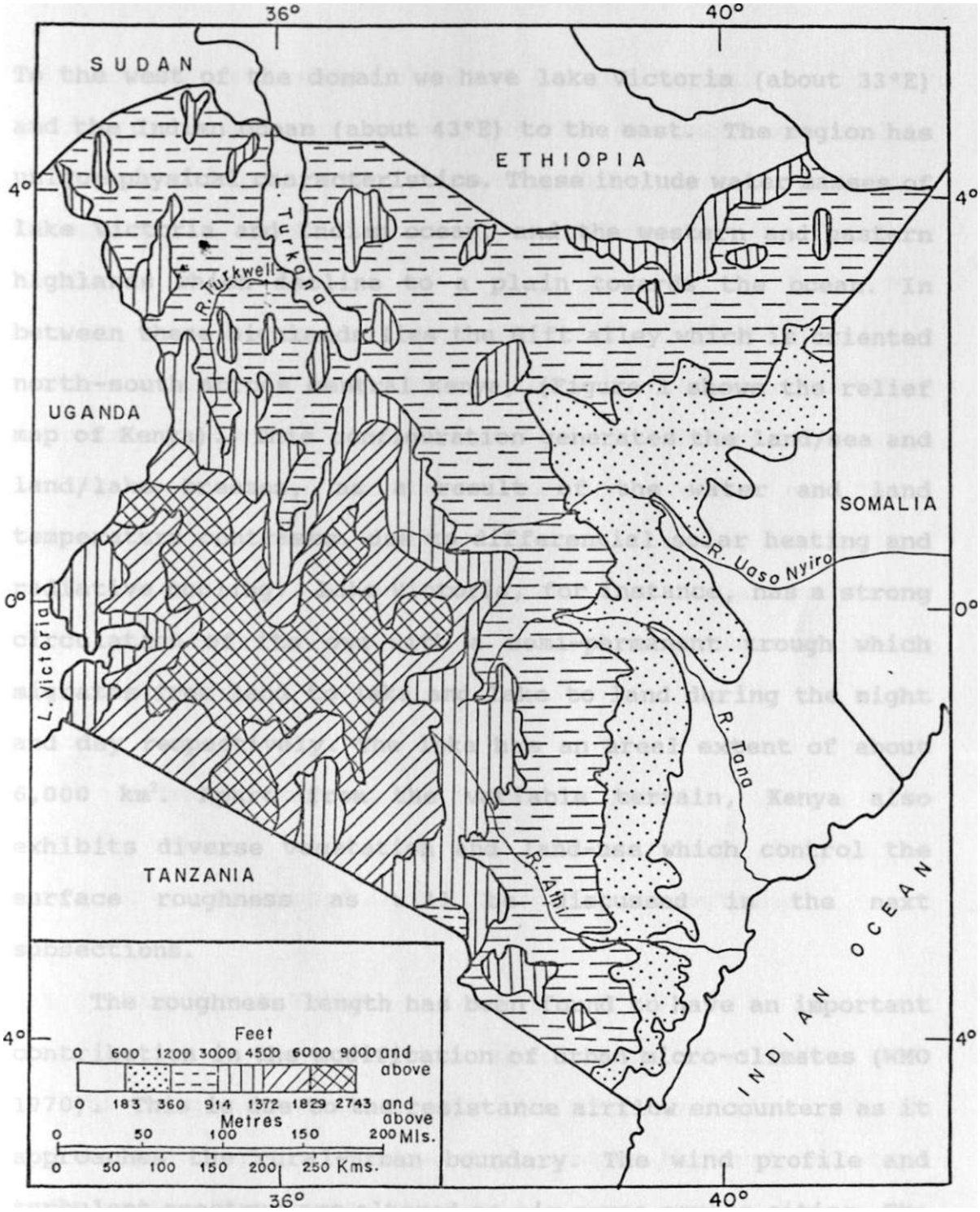

Fig. I Relief map of Kenya (Ojany and Ogendo, 1988)

To the west of the domain we have lake Victoria (about 33°E) and the Indian ocean (about 43°E) to the east. The region has unigue physical characteristics. These include water masses of lake Victoria and Indian ocean, and the western and eastern highlands which decline to a plain towards the ocean. In between these highlands lies the Rift alley which is oriented north-south across central Kenya, (Figure 1 shows the relief map of Kenya). This configuration generates the land/sea and land/lake breezes, as a result of the water and land temperature contrasts, due to differential solar heating and radiative cooling. Lake Victoria, for instance, has a strong circulation of its own with a semi-permanent trough which migrates from land to lake and lake to land during the night and day respectively. The lake has an areal extent of about 6,000 km^2. Apart from the variable terrain, Kenya also exhibits diverse vegetation and land-use which control the surface roughness as will be discussed in the next subsections.

The roughness length has been found to have an important contribution in the modification of urban micro-climates (WMO 1970) . This is due to the resistance airflow encounters as it approaches the rural-urban boundary. The wind profile and turbulent spectrum are altered as air moves across cities. The turbulent mixing in urban areas modifies the air guality through increased turbulence and induced micro-scale flows.

More frequent storms are observed in urban areas, as a result of increased moisture convergence due to increased surface roughness. Thus, heat moisture, momentum, and pollutant transport in urban areas is dependent on the surface roughness.

An increase in the roughness length leads to increased frictional drag, improved Ekman surface convergence and hence increased mixing and evaporation (Zhang and Anthes 1982). The strong evaporation results in surface cooling and hence reduces the surface heat flux. Factors affecting the surface roughness length in general and over Kenya in particular are both natural and anthropogenic as will be discussed in the next subsections.

1.2.0 FACTORS AFFECTING THE ROUGHNESS LENGTH

The factors that determine the roughness lengths of surfaces are discussed in the following subsections.

1.2.1 VEGETATION TYPES

Vegetation types and their spatial distribution are some of the major determinants of the characteristics of the surface over a given place, as they control the heat, moisture and momentum fluxes from the surface. Many studies have shown that vegetation influences the atmospheric circulation and precipitation, because vegetation affects the surface albedo

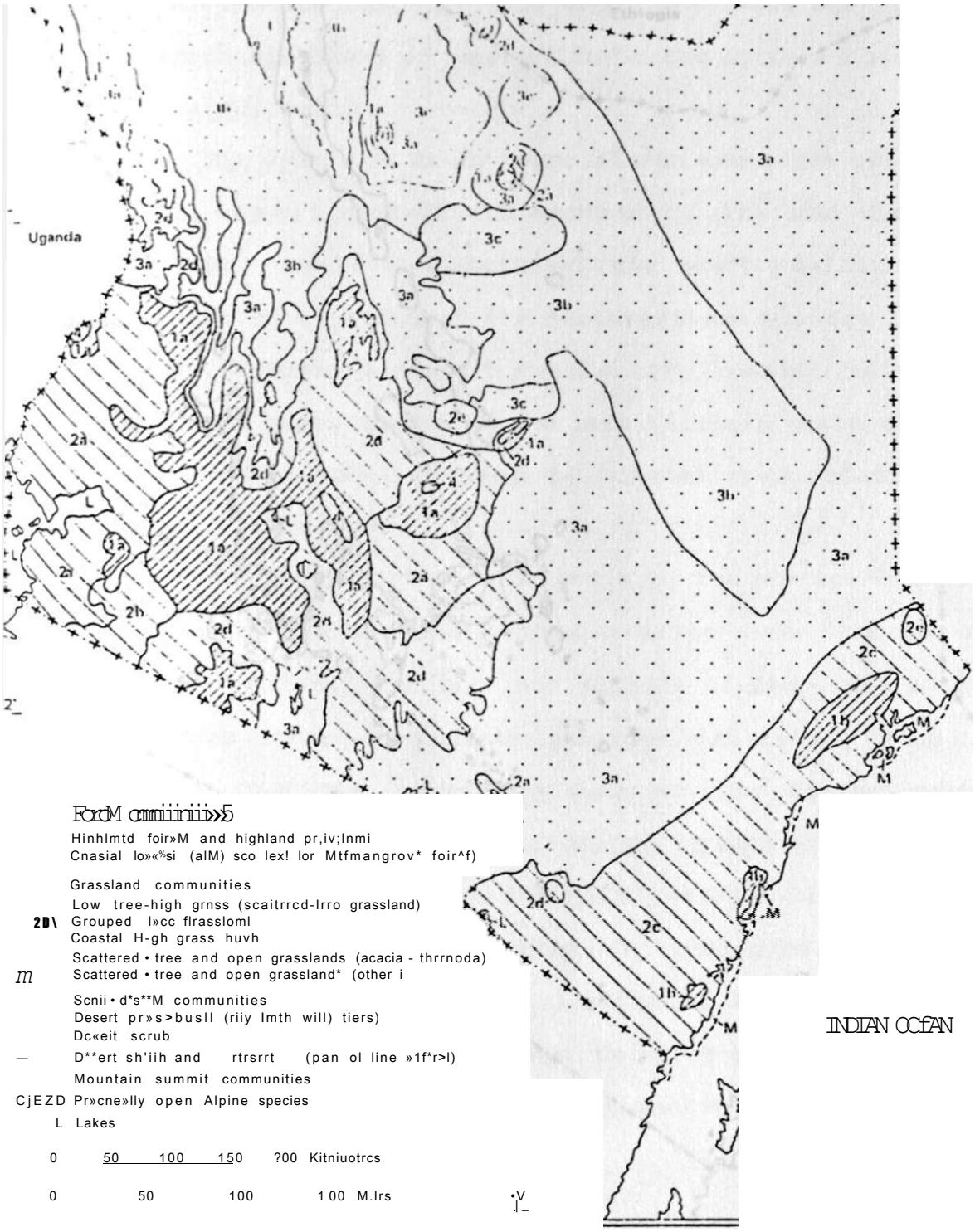

Pig. 2 Vegeto-ecological regions of Kenya (Ojany and Ogendo, 1988)

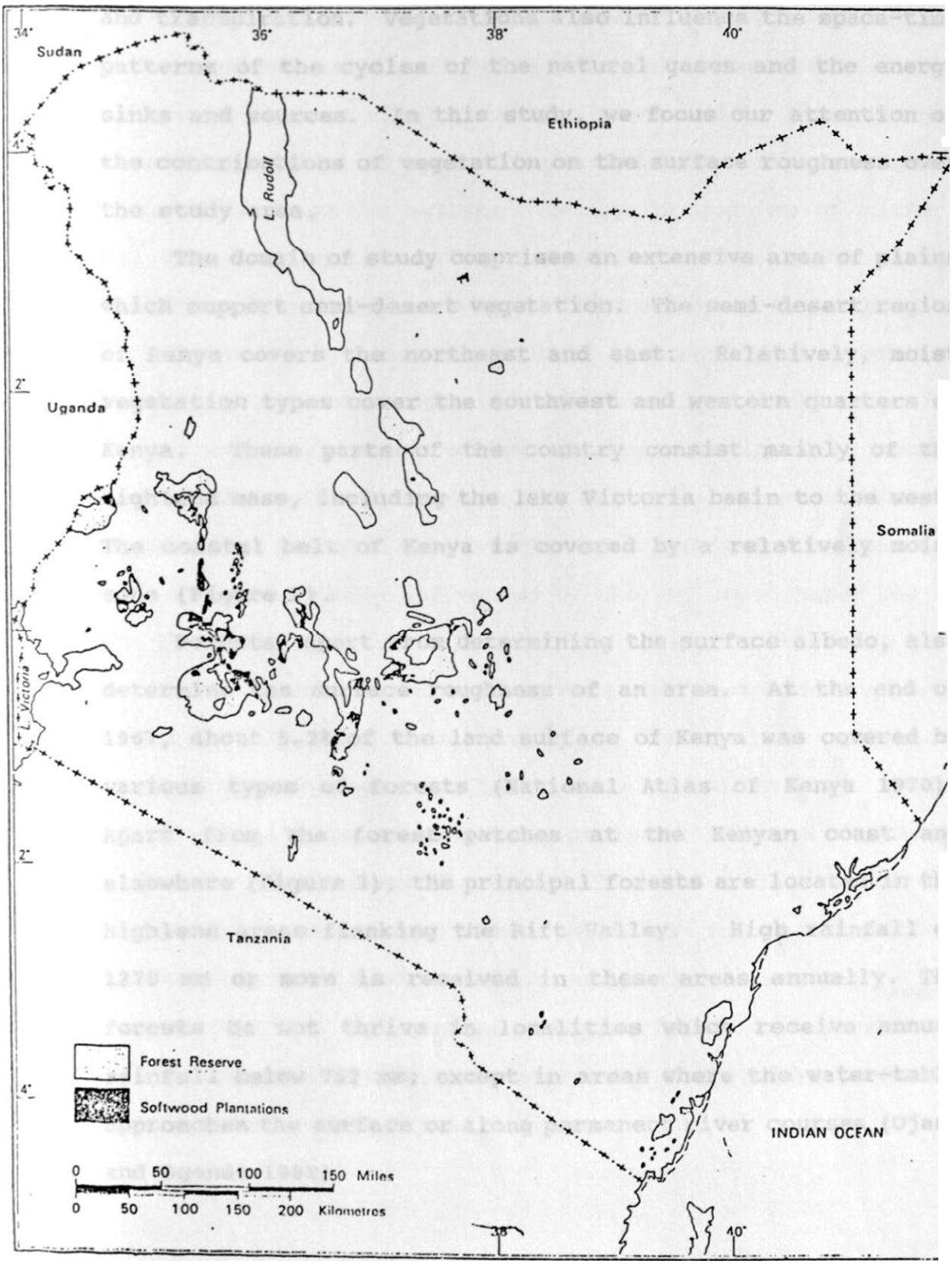

Fig. 3 Major forests of Kenya (Ojany'and Ogendo, 1988)

and transpiration. Vegetations also influence the space-time patterns of the cycles of the natural gases and the energy sinks and sources. In this study, we focus our attention on the contributions of vegetation on the surface roughness over the study area.

The domain of study comprises an extensive area of plains which support semi-desert vegetation. The semi-desert region of Kenya covers the northeast and east. Relatively, moist vegetation types cover the southwest and western quarters of Kenya. These parts of the country consist mainly of the highland mass, including the lake Victoria basin to the west. The coastal belt of Kenya is covered by a relatively moist zone (Figure 2).

Forests, apart from determining the surface albedo, also determine the surface roughness of an area. At the end of 1967, about 5.2% of the land surface of Kenya was covered by various types of forests (National Atlas of Kenya 1970). Apart from the forest patches at the Kenyan coast and elsewhere (Figure 3) , the principal forests are located in the highland areas flanking the Rift Valley. High rainfall of 1270 mm or more is received in these areas annually. The forests do not thrive in localities which receive annual rainfall below 762 mm; except in areas where the water-table approaches the surface or along permanent river courses (Ojany and Ogendo 1988).

About three quarters of the reserved forest area in Kenya is categorized as protective forests and is managed to ensure the protection of vital catchment areas and to prevent soil deterioration and adverse climatic changes. The importance forests in Kenya is measured through production of timber. All major irrigation schemes depend on water which partly originate from catchments in protective forest reserves.

It has been common in the past to present the vegetation types of Kenya as a compromise between that which actually occurs and that which ecological concepts indicate should occur. This situation has arisen not only because the Kenyan environment permits many vegetation types but also because most areas have been influenced by the prolonged human use in the form of grazing, burning, shifting cultivation and selective cuttings. Natural forests for instance have been reduced by cutting and burning to bushland or grassland converted by over-grazing to thickets or barren land. These past changes in vegetation patterns through land-use practices, deforestation, desertification and urbanization (rural-urban migration) have modified the land surface characteristics, such as albedo and surface roughness. The future temporal and spatial distribution of the vegetation will be important in the parameterization of surface processes in numerical models run over Kenya.

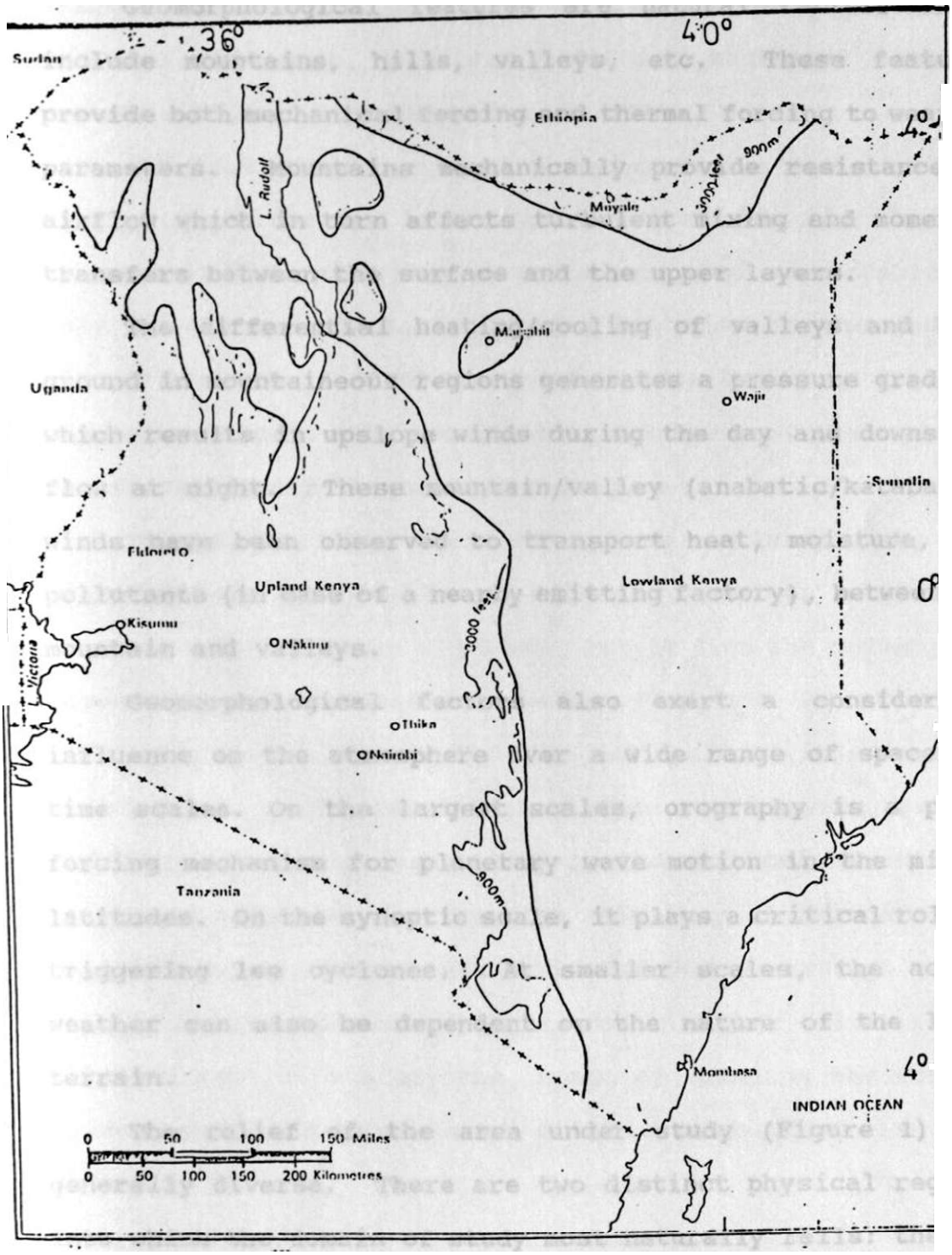

Fig. 4 Lowlands and highlands of Kenya (Ojany and Ogendo, 1988)

1.2.2 GEOMORPHOLOGICAL FEATURES

Geomorphological features are natural factors which include mountains, hills, valleys, etc. These features provide both mechanical forcing and thermal forcing to weather parameters. Mountains mechanically provide resistance to airflow which in turn affects turbulent mixing and momentum transfers between the surface and the upper layers.

The differential heating/cooling of valleys and high ground in mountaineous regions generates a pressure gradient which results in upslope winds during the day and downslope flow at night. These mountain/valley (anabatic/katabatic) winds have been observed to transport heat, moisture, and pollutants (in case of a nearby emitting factory), between the mountain and valleys.

' Geomorphological factors also exert a considerable influence on the atmosphere over a wide range of space and time scales. On the largest scales, orography is a prime forcing mechanism for planetary wave motion in the middle latitudes. On the synoptic scale, it plays a critical role in triggering lee cyclones. At smaller scales, the actual weather can also be dependent on the nature of the local terrain.

The relief of the area under study (Figure 1), is generally diverse. There are two distinct physical regions into which the domain of study most naturally falls: the

lowlands, which include all land below 915 m and highlands (Figure 4). Every land-form and land-scape (equatorial, tropical, savannah, glacial, volcanic, tectonic, etc) is present in Kenya (Ojany and Ogendo 1988).

The land rises very gently westward from the east upto about 915 m above sea level. Above this height, the climb to the west becomes much steeper and a more obvious obstacle not only to the transportation routes but also to the general flow. Mount Kenya (5200 m above mean sea level) an imposing composite volcano situated right in the heart of the country, is Africa's second highest peak (Figure 1).

Meso-scale flows over Kenya are influenced by the geomorphology of the area. Afternoon weather activities observed over the Kenya highlands, result from the convergence between the lake breeze and upslope flow from lake Victoria and the large-scale easterly flow and upslope winds from the Indian ocean. The resulting moisture convergence, coupled with the convective instability in the tropical atmosphere, provide a mechanism for the high frequency of the hailstorm over this area. It has been estimated that an average of 130 days of hailstorms occur in this area in a year (Alusa 1976). Our interest is to study the impact of changing the surface roughness in the development of this meso-scale flow over Kenya.

. 5 Major Urban Centres of Kenya (Ojany and Ogendo, 1988)

1.2.3 URBANIZATION

The highest value of the surface roughness is in the urban areas where man-made structures such as high buildings, have considerably modified the physical characteristics. This has in turn modified surface processes, albedo, roughness length and moisture availability.

The wind profile and turbulent spectrum is modified as air moves across cities. To add to the urban complexity, there is a rapid increase with height in the time and length of trajectory required for the wind to adjust itself to change of the surface roughness at the urban-rural boundary. It is assumed that winds are reduced in speed in urban areas though sometimes there may be an increase in the gusts. However, studies done in central London showed that in all seasons and by both day and night, light winds seem to increase in speed, a circumstance which is undoubtedly related to downward transport of momentum by mechanically induced eddies (WMO 1970). This momentum transfer induces micro-scale circulations in the urban areas.

In the presence of strong winds, there is a more gentle wind gradient in the boundary layer and the increase in surface friction in urban areas is then more important than the downwards transport of momentum. This leads to a general reduction in wind speed within the built-up area.

Urban centres in Kenya were started by the colonial

administration and traders. Urban areas in the country (Figure 5), are found mainly in the central parts and the productive western highlands. They include the administrative towns, the largest one being the capital city, Nairobi (largest city in East and central Africa), and provincial headquarters such as Mombasa. Mombasa is also the major port of the country. Most of the inland towns serve the farming community.

A high rate of population increase and the rural-urban migration of people in search of employment has led to the fast expansion of urban centres. This calls for a better understanding of the effect of the surface roughness changes induced by this urbanization, and the micro-scale circulation which may be generated in these areas (especially in the capital city, Nairobi). In this study we shall deal with the contribution of urbanization to changes in the roughness length. Efforts have been made to quantify the surface roughness for different surfaces as will be discussed in the following subsections.

1.3.0 QUANTIFICATION OF THE ROUGHNESS LENGTH

Results from experiments perfomed with general circulation models have shown that the atmosphere is sensitive to variations in processes at the land surface. Accurate parameterization of surface parameters is important for

predictions on time scales of a few hours or days to several months (Rowntree 1983, 1988). It is evidently important to represent land surface processes realistically. This requires adequate parameterization including specification of suitable data sets of vegetation, soil types, initial soil moisture, and general characteristics of the surfaces. The roughness length, albedo, vegetation index, emissivity, etc, are non-prognostic surface parameters which need initialization on long time scales (weekly or monthly), using satellite observations. On scales larger than 5 km the definition of roughness length and exchange coefficients become problematic because of inhomogeneous conditions. Hence meso-scale studies may be used to obtain a better evaluation of these quantities.

Several researchers have made attempts to quantify the roughness length depending on the physical features of different surfaces. The evaluation of an effective areal surface roughness for heterogeneous surface is an important practical issue that is yet to be resolved satisfactorily. The effective areal z_G for natural surfaces is rarely estimated from wind profile and/or surface shear stress measurements. Instead, it is usually determined indirectly from a knowledge of factors such as terrain relief (geomorphological features of the given area), land use, and type and distribution of the surface roughness elements. In many models discussed by Carson (1986), roughness dependence

were ignored. In the absence of vegetation data sets the spatial variations of the roughness parameter were neglected, a constant z_Q being assumed (Okeyo 1982) . Hansen et al. (1983) introduced vegetation dependence of z_0 which has been included in many climate models.

Early numerical modelers used simple parameterization schemes that lacked geographical variations of most surface characteristics. More complex schemes have however, been developed in recent years. Firstly, geographical variations of a few important surface parameters such as albedo, roughness parameter and root depth were introduced (Hansen et al. 1983), then more elaborate and hopefully more realistic parameterization have been developed by Sellers (1986), Sellers et al. (1988), and Carson (1990).

Fiedler and Panofsky (1972) defined an "effective" roughness length for use over heterogeneous terrain as the roughness length which homogeneous terrain would have in order to give the correct surface stress over a heterogeneous area. In order to estimate the effective roughness length, Fiedler and Panofsky (1972) measured the average stress near the ground over the heterogeneous area, and then applied the theory of wind profile for neutral airflow over homogeneous terrain to derive the roughness length, which was then assumed constant. The method used was however, tedious and expensive as they had to use aeroplane to estimate the

Tabled Effective mesoscale surface roughness length, z_0 (m), expressed as a function of land use and proposed by Wleringa (1986). H Is the height of the major surface obstacles.

Land use category	z_0
Sea (minimal fetch 5 km)	0.0002
Small lake, mud flats	0.006
Morass	0.03
Pasture	0.07
Dunes, heath	0.10
Agriculture	0.17
Road, canal (in Dutch landscape tree-lined)	0.24
Orchards, bushland	0.35
Forest	0.75
Residential built-up area (H < 10 o)	1.12
City centre (high-rise building)	1.6

turbulence statistics of the area in question. In their study, Fiedler and Panofsky estimated the effective roughness lengths as 0.42, 0.99, and 1.42 m for plains, low mountains, and high mountains respectively.

Pielke (1974) used the friction velocity (u*) and gravitational force (g) to compute z_0 for water surfaces, using the equation $z_o=0.032u*/g$, with the requirement that $z_Q > 0.0015$ cm. The dependence of z_Q on frictional velocity (u*) and gravitational force (g) was first suggested by Charnock (1955) . Garrat (1977) has reviewed the estimates of the roughness parameter for different surfaces. He noted that values of z_0 fall in the range $0.02 < z_0/h < 0.2$, where h is the height of the roughness elements, and estimated values which range from 0.0003 m, for desert to 1.5 m, for forests.

Most standard boundary layer text books provide a table of values of z_0 as a function of terrain type described qualitatively in terms of relief and vegetation characteristics. Such traditional relationships may be adequate on the very local scale for smoother, quasi-homogeneous types of terrain, but may not be appropriate for rough, heterogeneous terrain typical of Kenya. In urban areas, where the roughness increases towards the down-town area and then diminishing again, it is not possible to estimate the roughness length accurately. Furthermore, there may be open areas such as parks, or small clusters of high

rise apartments, surrounded by residential areas. Weiringa (1986) has addressed this problem and produced a table giving effective areal z_Q in terms of terrain classification where there is no significant orographic effects (Table 1) . For more techniques of evaluation of effective z_0 reference can be made to Andre and Blondin (1986).

Numerical studies so far done over Kenya have only considered modelling aspects of meso-scale systems and their influence on weather patterns over Kenya (Okeyo 1982, 1987). However, the response of these models to changes in surface parameters have not been investigated.

Okeyo (1982) considered a roughness value of 5 cm to represent the entire domain of his study but suggested that the influence of surface parameters be tested to find out their contribution in the development of meso-scale systems over Kenya. This would lead to more accurate specification of these parameters.

In the next subsection, we define the objective of the study.

1.4.0 OBJECTIVE OF THE STUDY

The main objective of this study will be to investigate the effects of changes in the roughness length on the development of meso-scale flow over Kenya, based on a numerical simulation. The results are expected to be used in

future for establishing an effective roughness length for use in meso-scale numerical models run in Kenya. Although this study focuses on meso-scale developments, it should be noted that the large-scale flow is important in determining the intensity and location of the meso-scale convergence. However, the incorporation of large-scale flow is beyond the scope of the present study.

In order to achieve the objective, a meso-scale numerical model developed by Anthes et al. (1978) and modified by Okeyo (1987) will be used. Details of this model are given in the next chapter. The indices of the roughness length will be established for different regions of Kenya as defined by Fiedler and Panofsky (1972), and Weiringa (1986), (Table 1). This work will contribute to the improvement of weather forecasting in Kenya, from the traditional practice of chart analysis.

In the next subsection, we review the previous literature related to the present study.

1.5.0 LITERATURE REVIEW

Most studies on the sensitivity of atmospheric circulation to varying surface parameters such as roughness length use General Circulation Models (GCM's). Since meso-scale circulations play a major role on the weather experienced in Kenya, we have opted to use Limited area model

in this study.

The area of study has a diverse topography, vegetation and land-use with meso-scale flows controlling the weather patterns, hence an understanding of the impacts of the roughness length among other surface parameters, on their development is important.

Pielke (1974) examined the effect of roughness on meso-scale (land/sea breeze) flow over south Florida and concluded that the differential roughness between land and water does not by itself play an important role in the magnitudes of convergence. Indirectly, however, the surface roughness has an influence on the magnitudes of convergence through the increased turbulent transfer of heat. This effect has to be included in any numerical model of the sea-breeze.

Rainfall over and adjacent to the Sahara desert was found to be sensitive to the roughness of the desert surface (Sud et al. 1985a). Surface roughness has also been found to have a large influence on the summer rainfall over India, and that influence is as important as that of surface albedo (Sud et al. 1985b).

Sud et al. (1988) showed that the reduction in surface roughness produced about a two-fold increase in the boundary layer wind-speed and at the same time a two-fold decrease in the magnitude of the surface stress. There was no change in the surface evaporation and surface sensible heat flux. There

was however, a large change in the horizontal convergence of water vapour transport in the boundary layer and a corresponding large change in the rainfall distribution mainly as a conseguence of the change in the curl of the surface stress. Their results suggested that the height of the earth's vegetation cover, which is the main determinant of the land surface roughness, has a large influence on the boundary layer water vapour convergence and the rainfall distribution. Surface parameters as discussed above control the exchange of moisture, momentum and heat fluxes in the planetary boundary layer. Little has been done on the effects of the changes in the roughness length in the meso-scale circulations, especially in the eguatorial regions where the coriolis force (f=2nsina>) is negligible, and the development of meso-scale flow is mainly generated by the horizontal temperature contrasts. In this study, we investigate the impacts of the changes in the roughness length on the development of meso-scale flow over Kenya which lies astride the eguator.

In the following subsections, we highlight the general climate of Kenya.

1.6.0 THE CLIMATE OF KENYA

Kenya is bounded by the Indian ocean to the east (at a level of about 10 m Amsl) , and lake Victoria (the largest lake in the tropics and the second largest in the world) , to the

west. The northern parts of Kenya are dominated by semi-arid to arid areas. The East African highlands in the central parts of Kenya are mainly covered with forests. The great Rift Valley which is 60 km wide and 330 m deep also passes through the country. A large part of this Valley is occupied by range-lands (Ojany and Ogendo 1988) .

Since the country lies astride the equator, one would expect it to have an equatorial type of climate. The region however, has a wide range of climate characteristics which include hot deserts, polar climate at the top of mount Kenya, equatorial climate and many others. Bimodal rainfall regime is however common over many areas associated with the double passage of the Intertropical Convergence Zone (ITCZ), which lags behind the over head-sun (Anyamba 1983, Ogallo 1984).

Some of the large-scale systems which affect the meso-scale convergence and weather in the domain of study are discussed in the next subsection.

1.6.1 SOME INFLUENCE OF LARGE-SCALE FLOW ON MESO-SCALE FLOW IN KENYA

Meso-scale flows over Kenya include the land/lake breezes over western highlands of Kenya, the land/sea breezes along the coast and upslope/downslope winds. These meso-scale flows are generated by the temperature contrasts, due to heating from the sun and radiative cooling at night. The varied

topography over Kenya also plays an important role in determining the characteristics of these meso-scale flows. The contrast between the diurnal variations in thunderstorm activity at Kisumu (Lat. 0° 06'S, Long. 34° 45'E) on the eastern shore and Entebbe (Lat. 0° 03'N, Long. 32° 27'E) on the western shore of lake Victoria has been found to be due to the local topography of the area (Lumb 1970) . Rainfall, hail and thunderstorms observed over the western highlands of Kenya in the afternoon and night and early morning rains observed over the coastal areas and the eastern highlands have been attributed to the interaction between the meso-scale flows and the large-scale flow (Majugu 1983). Majugu (1983), in his observational study of the mean and seasonal diurnal variation of precipitation in East Africa, found that the highlands of Kenya receive as much as 40% of the day's rainfall in the late afternoon, between 1600 and 1900 hrs local time. Asnani and Kinuthia (1979) observed that the highlands receive minimum rainfall in early to late morning (0500 hrs to 1100 hrs local time).

Kenya experiences two monsoon systems in a year: the northeast (NE) monsoon (December-February) and Southeast-Southwest (SE/SW) monsoon (June-August) of the Northern Hemisphere winter and Summer respectively. There are two transition periods between these monsoons: one in March to May and the other in September to November. During these periods,

the winds are more fickle and easterly. These are the periods when Kenya experiences the "long" (March-May) and "short" (Oct.-Nov.) rains respectively. The Northeast monsoon which emanates from the Arabian anticyclone to the north is shallow, highly diffluent and generally dry (Findlater 1971). Hence, this NE monsoon has less influence on the meso-scale circulations over Kenya. The SE/SW monsoon emanates from the Mascarene anticyclone in the southweast Indian ocean. It is characterized by the presence of the East African low-level jet (EALLJ), (Findlater 1971), and is associated with the northern summer cross-equatorial air current over the west Indian ocean which has important contribution towards the inter-hemispheric mass and energy exchange. The SE/SW monsoon season is generally dry over most parts of Kenya, with a few areas over western parts of Kenya experiencing wet conditions (Tomsett 1969). These rains over western Kenya have been explained as being due the interaction between the southeast monsoon current and the lake Victoria thermally induced meso-scale circulation (Asnani and Kinuthia 1979). Kericho, in western Kenya has been observed to have one of the highest frequency of occurrence of hail storms in the world (Sansom and Gichuiya 1971, Alusa 1976). During the day, the lake breeze and upslope winds from the west and the sea breeze, upslope winds and the generally easterly current from the east converge to the east of Kericho/Nandi Hills area, resulting in

severe thunderstorms and hail that move westward with the general easterly flow to hail over Kericho.

During the transitional periods, the NE and SE trades converge in the intertropical convergence zone (ITCZ) over Kenya. The confluence between the trades is diffuse and is hardly detectable on the daily weather charts. The diffuse nature of the ITCZ has been attributed to the local orographic influences. The ITCZ over Kenya exhibits diurnal oscillations due to the changes in the surface pressure distribution. These diurnal changes, as pointed out by Sansom (1963), are more pronounced in areas of strong meso-scale circulations such as the lake Victoria region.

Apart from the monsoon winds, westerly winds, observed at the altitude of 2-3 km AMSL in East Africa have been associated with active weather conditions. It is believed that occasions of deep westerlies are more productive of rain than those when easterlies prevail (Johnson and Morth 1960). These westerlies are generally unstable and moist, and originate from the moist Congo forest. The relative wetness over the western parts of Kenya has been attributed to the incursion of westerly winds. The meso-scale circulations over the western parts of Kenya are greatly influenced by these westerlies. It is believed that the afternoon convergence over the western highlands is accompanied by intense precipitation during occasions of moist westerlies from Congo

forest (Majugu 1983).

Apart from the westerly winds, easterly waves also influence climate and weather over Kenya. These waves can be described as westward propagating wave-like perturbations within the easterly current on the equatorward sides of the subtropical high pressure belts. These waves are generally feeble features that are not easily noticed on synoptic charts where quasi-permanent synoptic systems are dominant. Njau (1982), detected westward propagation of the easterly disturbances with a maximum intensity in the lower and middle troposphere. The coastal belt of Kenya experiences more early morning rains in the pressence of an instability off the coast in the Indian ocean. This is due to the increase in the advected moisture in the easterly current. These rains however, do not penetrate more than 80 km inland. This has been attributed to pronounced diffluence in the low-level monsoon current over the East African coast (Thompson 1957). Not much work has been done on the interaction of Easterly waves and the meso-scale flow over Kenya. It will be of interest for this study to be done in future.

In the next chapter we discuss in detail the model used in this study.

CHAPTER 2

2.0 NUMERICAL MODEL FORMULATION AND DESIGN OF EXPERIMENTS

The model used in this study is a three dimensional meso-scale numerical model which was developed by Anthes and Warner (1978). This model has been modified to incorporate parameterization of cumulus convection, full physics and dynamics of both the meso-scale and convective scale systems over Kenya by Okeyo (1987). Details of the model are provided in the following sections.

2.1 DOMAIN AND GRID STRUCTURE

The domain of integration was bounded by 33°E to 43°E longitudes and 5°N to 5°S latitudes. The lateral spacing was 111.1 km (l°x 1°) in both East-West and North-South directions. There were 11 grid points in the X and Y directions and 10 sigma levels in the vertical. The vertical coordinate of the model is the terrain-following sigma (CT) coordinate, defined as:

where P"=P,-P_t, P is the pressure at any level, P_s is the pressure at the surface, and P_t is the pressure at the top of the model atmosphere.

2.2 THE MODEL EQUATIONS

The numerical model equations are given below in equations (4) to (13). The model uses a terrain following vertical coordinate (a) and the Mecartor map projection. This map projection maps almost one to one over the equatorial region and is given by:

$$m = \frac{\overline{\quad}}{\cos 0} \hat{} \tag{3}$$

where 6 is the latitude and 6_0 the latitude at which the projection is true (usually $6_0 = 0$ at the equator) .

The zonal and meridional components of the momentum equation are given in equation (4) and (5) respectively while the continuity, thermodynamic and moisture equations are given in (6) , (7) and(8) .

$$\frac{\partial up^*}{\partial t} = -\left(\frac{duup'}{dx} \hat{} \frac{duvp'}{dy} \right) \_ \frac{duap}{da} \sim P \left\{ \frac{RT}{(p^* + \frac{p_t}{\sigma})} \frac{\partial p^*}{\partial x} + \frac{\partial \phi}{\partial x} \right\} + p^* fv + F_H U \tag{4}$$

$$\frac{dyPlJ}{dt} \{ \frac{\partial uvp^*}{\partial x} \frac{\partial vvp^*}{\partial y} \Big) - \frac{\partial v\dot{o}p^*}{\partial \sigma} \sim P \quad \left\{ \frac{RT}{p_{t\hat{}}} \frac{\partial p^*}{\partial y} + \frac{\partial \phi}{\partial y} \right\} - p^* fu + F_H V$$

(p*- —i

(5)

$$\frac{\partial p^*}{\partial t} = -\left(\frac{\partial p^* u}{\partial x} + \frac{\partial p^* v}{\partial y} \right) - \frac{\partial p^* \dot{\sigma}}{\partial \sigma} \tag{6}$$

$$\frac{dp'T_m}{dt} J \left(\frac{dup'T_+}{dx} \; \underline{3vpT\hat{}}{dy} \; \_ \right) \frac{dp'To_+}{do} \qquad \underline{RTu} \; {}_+P10_{+F} \; q_H$$

$$Cp\,(p^{*+}\,\underline{p_t.}{}_o\sim)\qquad c_D$$

(7)

(8)

The vertical velocity in sigma coordinates (a) is computed at each level in the model from the equation:

$$p'J \; i \; at \qquad dx \qquad dy \; j$$

(9)

where a' is a dummy variable of integration and a(a=0)=0. The vertical motion, co is given by:

$$at$$

(10)

where

$$dt \quad dt \qquad dx \qquad dy$$

(11)

The hydrostatic equation is used to compute the geopotential heights from the virtual temperature T_v, and is given by:

$$\underline{d\Phi} \quad \_\_ \quad \underline{RT_V}$$

$$P* \qquad I \qquad 1+Qy$$

(12)

where T_v is given by:

$$T_V = T(1 + 0.608 g_v) \quad (13)$$

and q_v, g_c and g_f are the mixing ratios of water vapour, cloud water and rain water respectively.

2.3 THE WATER CYCLE

There are three options for treatment of the water cycle in the model. The first option is a dry one where water vapour is treated as a passive variable. In this option, latent heat of condensation is not added into the thermodynamic equation. In the second and more general option, prognostic equations for water vapour, cloud water, and rain water are included. This scheme is called the explicit scheme and follows Hsie et al. (1984). In the last scheme, cumulus parameterization following Kuo (1974) and Anthes (1977) is used. In this scheme, the total convective heating is proportional to the moist convergence in a column while the distribution of convective heating in the vertical is computed from an estimate of the convective cloud base and top and an assumed functional form.

Okeyo (1987), considered all these options and recommended cumulus parameterization in the simulation of meso-scale flows over Kenya. In this study we use cumulus parameterization scheme similar to that used by Anthes et al. (1987). The vertical heating profile is prescribed following

Yanai et al. (1973). The total amount of convective rainfall is determined by moisture convergence within a grid column. In this scheme the equations of heat and moisture are given as:

$$P \qquad (14)$$

$$dR\hat{}=gbM_cN_a(o) + V_{qf}(a) + FQ \qquad (15)$$

where N_h and N_m are respectively non-dimensional convective heating and moistening profiles and V_{qf} is the vertical flux divergence of moisture by cumulus convection. The integrated moisture convergence is defined by:

$$\int_0^I \qquad (16)$$

A portion (1-b) of M, is assumed to condense and fall as rain, while the other portion (b) is used to moisten the column. Hence,

$$\int_0^I Jp'c'da = (1-b)\, gM_t \qquad (17)$$

where c* is the net condensation rate averaged over a grid volume.

Table 2 Description of land-use categories and physical parameters for summer (15 April-15 October) and winter (15 October-15 April).

Landusc Integer Identification	Landuse Description	Albedo (%)		Moisture Avail. (%)		Emissivity (% at 9 um)		Roughness Length (cm)		Thermal Inertia (cal enr^2 K-' s$^{1/2}$>	
		Sum	Win	Sum	Win	Sum	Win	Sum	Win	Sum	Win
1	.Urban land	18	18	5	10	88	88	50	50	0.03	0.03
2	Agriculture	17	23	30	60	92	92	15	5	0.04	0.04
3	Range-grassland	19	23	15	30	92	92	12	10	0.03	0.04
4	Deciduous forest	16-	17	30	60	93	93	50	50	0.04	0.05
5	Coniferous forest	12	12	30	60	95	95	50	50	0.04	0.05
6	Mixed forest and wet land	14	14	35	70	95	95	40	40	0.05	0.06
7	Water	8	8	100	100	98	98	.0001	.0001	0.06	0.06
8	Marsh or wet land	14	14	50	75	95	95	20	20	0.06	0.06
9	Desert	25	25	2	5	85	85	10	10	0.02	0.02
10	Tundra	15	70	50	90	92	92	10	10	0.05	0.05
11	Permanent ice	55	70	95	95	95	95	5	5	0.05	• 0.05
12	Tropical or sub-tropical forest	12	12	50	50	95	95	50	50	0.05	0.05
13	Savannah	20	20	15	15	92	92	15	15	0.03	0.03

N_m is defined as:

$$\int_0^{\infty} q_s(a)\, da \qquad (18)$$

where q, is saturated mixing ratio. Both $N_h(a)$ and $V_{qf}(a)$ are prescribed functions of a, with the constraints:

$$\int_0^{\infty} N_h(o)\, do = 1 \qquad (19)$$

and

$$\int_0^{\infty} V_{qt}(a)\, da = 0 \qquad (20)$$

In this scheme cumulus convection is activated when $M, > M_c$ where M_c is a critical value of moisture convergence (usually taken as 3.0×10^{-5} kgm^{-2}s^{-1}) . Computation of $N_h(a)$ has been discussed by Yanai et al. (1973) and Kuo and Anthes (1984a). V_{qf} is estimated assuming a vertical profile of cloud vertical motion (a_c) and q', the deviation of cloud mixing ratio $q_{c>}$ from the environmental mixing ratio q.

2.4 SURFACE ENERGY FORMULATION

Over land, the surface temperature T_g is computed from the surface energy budget, following the slab model developed by Blackadar (1979).

The equation is given as:

$$C_g \frac{\partial T_g}{\partial t} = R_n - H_m - H_s - L_v E, \quad (13)$$

where C_t is the thermal capacity per unit area of the slab ($J m^{-2} K^{-1}$), R_n the net radiation, H_m the flow into the substrate, H, the sensible heat flux into the atmosphere, Ly the latent heat of evaporation, and E, the surface moisture flux. Blackadar (1979), showed that the following formulation enabled the amplitude and phase of the slab temperature to be identical to the surface temperature variation of a real soil layer of uniform thermal conductivity X and heat capacity per unit volume C_s. C_g is related to these parameters and the angular velocity of the earth fl by:

$$C_g = 0.95\left(\frac{\lambda C_s}{2\Omega}\right)^{1/2} \quad (22)$$

and the thermal capacity C_g is related to thermal inertia X BY:

$$C_{ff} = 3.293 \times 10^{6} X \quad (23)$$

where

$$x = ac_g)^{1/2} \quad (24)$$

is expressed in units of cal cm^k's'"^{2} and is specified as a function of land-use characteristics (Table 2).

This scheme was found by Deardorff (1978) to be superior to five other schemes in computing ground temperature and heat flux.

2.5 BOUNDARY LAYER FORMULATION

There are two approaches to the representation of vertical transports in the planetary boundary layer (PBL). The first approach is the bulk type of parameterization in which the PBL is represented by a single layer and the fluxes of heat, moisture and momentum are related to the surface conditions and the temperature, humidity and momentum variables at the lowest model level through exchange coefficients. Although this scheme is efficient computationally and is suitable for many purposes, it may not be adequate for systems that depend critically on the vertical details of the flow and stability in the PBL.

The second approach is to use a high resolution model. In this approach the structure of the PBL is resolved explicitly by including several computational levels within the boundary layer. High resolution PBL formulation was reviewed by Blackadar (1979). The high resolution approach is suitable for systems whose vertical variations of the wind, temperature and moisture in the lowest layers are of major concern. Such systems include flow over complex terrain similar to the one in Kenya, sea and land breezes, urban heat

island flows, flows under strongly baroclinic situations, and flows in which a strong gradient of water vapour exists.

In this study, we adopt a high resolution PBL model developed by Blackadar (1979) and described by Zhang and Anthes (1982) and Anthes et al. (1978). In this approach the surface heat and water-vapour fluxes are computed from similarity theory. Firstly, the frictional velocity u* is computed according to:

$$u* - MAX \quad Uo \quad \text{lnt-^S)-*.} \tag{25}$$

where $u*_G$ is a background value (0.1 ms'^1 over land and zero over water). Other symbols are defined in the list of symbols.

V is given by:

$$v=\{vl + vl)^{1/2} \tag{26}$$

where V, is the wind speed at the lowest model level and V_c is a "convective velocity", which is important under conditions of low mean wind speed and unstable conditions:

$$V_c - C(6 - 6.)^{1'^2}, \quad (8 \pounds 0_a) \tag{27}$$

$$v_c=o \ <e_{ff}<ej \tag{28}$$

C is equal to 2.0 ms 'k'"^{2} and 6 and 0„ are potential

temperature for ground and lowest model layer respectively. The surface heat flux is computed from:

(29)

where T* is given by:

$$T^* = \frac{\theta - \theta}{1} \quad g$$

(30)

z_0 is the roughness parameter, z, the height of the lowest a-level, and ψ_m and ψ_b are nondimensional stability parameters that are a function of bulk Richarson number R^, which is given by:

$$O \_ 9^{Z} a \frac{^{e}va" ^{e}vg}{V^2} \quad .C^vaj^$$

(31)

The subscript v represents virtual potential temperature, while other variables are defined in the list of symbols. There are four cases possible:

Case 1: Stable

where R^ is a critical Richardson number (=0.2)
In this case,

$$u' = u_r$$

(28)

••-•..--lOln

(33)

I -25 *Mm~²* *J*

(34)

Case 2: Mechanically Driven Turbulence

0 < R_{iB} < R_{ic}

IM)

(35)

Case 3: Forced Convection

RiB < 0 and |h/L| < 1.5

where L is the Monin-Obukhov length defined by:

(36)

and h is the height of the PBL. In this case,

(37)

Case 4: Free Convection

R_B < 0 and |h/L| > 1.5,

and z,/L is restricted to be no less than -2.0. For z./L equal to -2.0, = 2.29 and \j⁄m = 1.43. Anthes et al.

(I)

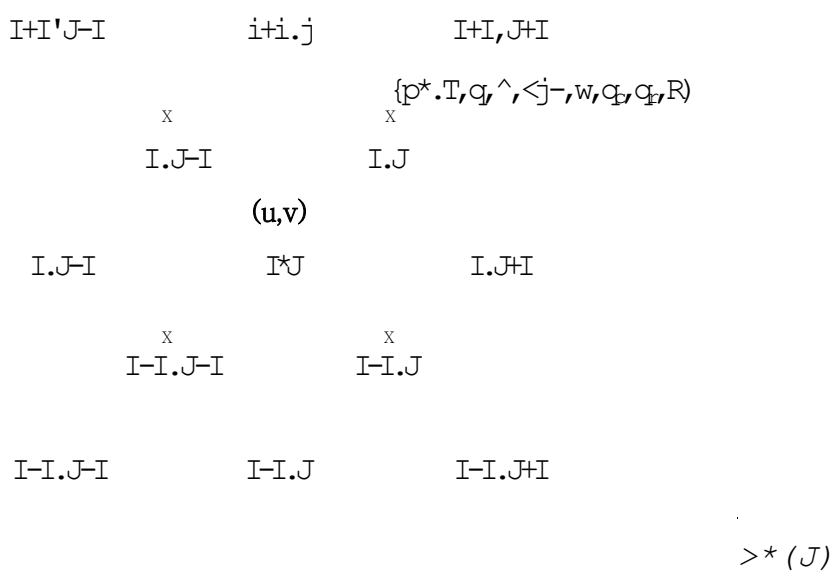

Fig. 6 Horizontal grid structure in the model

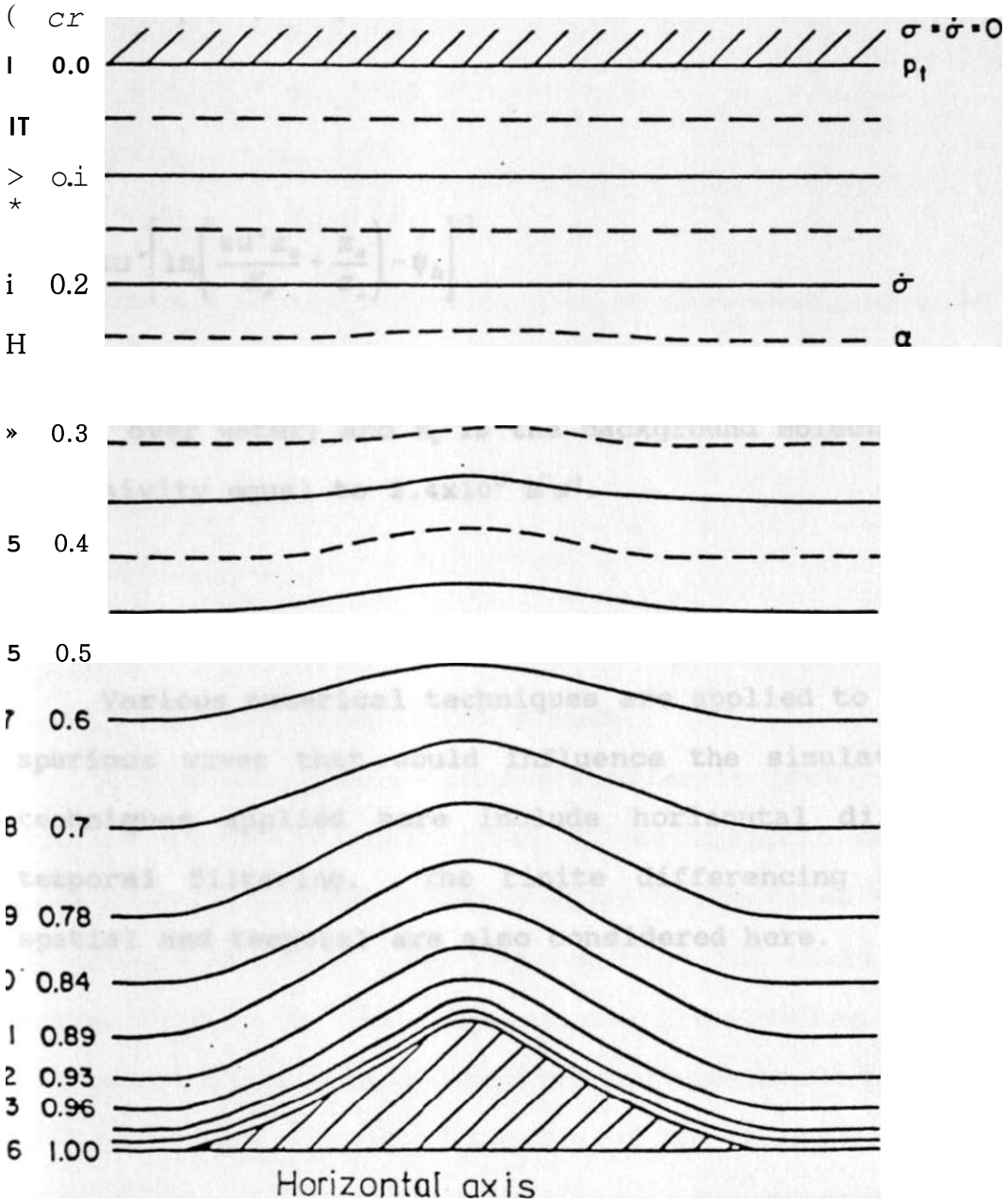

r* 7 Vertical grid ilructure In tie model. The variable a li defined •(the full" model levels. I other variable*, repreiented by o, are defined al the •half" level«.

(1987), have discussed in detail the computation of ^ and

The formulation of the surface moisture flux in this case was derived by Carlson and Boland (1978):

$$E. = M p_{11} I^{-*} [q, (T_g) \sim q_a] \tag{38}$$

where

$$I \quad -KU^{*} \ln \frac{KU\ z_{\wedge}}{K,} 2 + \frac{z_{\star}}{} \quad -1 \tag{39}$$

z, is the depth of the molecular layer (0.01 m over land and z_c over water) and K, is the background molecular diffusivity equal to 2.4x10"^{5} m^{2}s"'.

2.6.0 NUMERICAL TECHNIQUES

Various numerical techniques are applied to control the spurious waves that would influence the simulations. The techniques applied here include horizontal diffusion and temporal filtering. The finite differencing scheme both spatial and temporal are also **considered** here.

2.6.1 FINITE-DIFFERENCE SCHEME

The finite difference scheme used in this study is similar to that used by Anthes and Warner (1978). The finite-difference operators are given as:

$$
\begin{aligned}
a_x &= (a_{ij+1/2} - a_{ij-1/2})/\Delta x \\
a_y &= (a_{i+1/2,j} - a_{i-1/2,j})/\Delta y \\
a^x &= (a_{ij+1/2} + a_{ij-1/2})/2 \\
a^y &= (a_{i+1/2,j} + a_{i-1/2,j})/2
\end{aligned}
\qquad (40)
$$

where a is any variable, j is an east-west index and i is the north-south index. The vertical differences and averages are defined as:

$$
\begin{aligned}
a^0 &= (a_{k+1/2} - a_{k-1/2})/2 \\
\delta a &= (a_{k+1/2} - a_{k-1/2})
\end{aligned}
\qquad (41)
$$

2.6.2 TEMPORAL INTEGRATION SCHEME

A time-integration scheme similar to that of Brown and Campana (1978) is used. This is an explicit scheme which permits for a time step nearly equal to two times that allowed by the conventional leapfrog scheme. The stability of the scheme depends on the computation of the values of p' and co at time-step r+1 before computing the momentum values at time-step **T** + 1. Then a weighted average of the values of p* and **A>** at time-steps **T-1** and r**+1** are utilized in the pressure gradient

force terms equations (1) and (2); i.e., the p* in these equations is:

$$P^{*=T?}\ (P^{*M} + p^{v+1}) + (1\sim 2r])p'^{T} \qquad (42)$$

with a similar expression for **CJ.** The scheme is stable for rj<0.25 and permits maximum time-step for 0.25. In this study a value of **TJ**=0.2495 is used following Anthes and Warner (1978) and Anthes et al. (1987) .

A frequency filter (Asselin 1972) is applied to all prognostic variables in order to reduce the amount of energy in waves with high freguencies.

2.6.3 HORIZONTAL AND VERTICAL GRIDS

A staggered grid system similar to one described by Anthes et al. (1987) is used. The horizontal velocity components are defined at full grid (dot) points while the other variables are defined at half grid (cross) points (Figure 6) . The vertical grid is staggered with horizontal velocity components, geopotential and pressure defined at same levels while vertical velocity («) is defined at adjacent levels (Figure 7).

2.6.4 HORIZONTAL AND VERTICAL DIFFUSION

Horizontal and vertical diffusion is necessary in the model to control nonlinear instability and aliasing. The two types of diffusion used in this model are - a second-order diffusion of the form:

$$F_{H2}a=p*K_f y_o a \tag{43}$$

where a is a prognostic variable, and a more scale-selective fourth-order diffusion of the form:

$$F_{B4}a = -p'K\hat{}_a a \tag{44}$$

where

(45)

As is the grid size. The second-order diffusion form is used for the rows and columns of grid points next to the lateral boundaries and in vertical diffusion computations, while the fourth-order diffusion form is used on the interior of the horizontal grids.

2.7.0 INITIAL AND BOUNDARY CONDITIONS

Two parameters which are critical in any numerical simulation are initial and boundary conditions.

2.7.1 INITIAL CONDITIONS

Initial conditions in a numerical simulation represents the space-time characteristics of the atmosphere at the beginning of the numerical experiment.

Meso-scale atmospheric disturbances considered in this study have a temporal scale of a few hours to one day, and spatial scales of 1 km to about 200 kilometers, and their solutions are often more dependent on local forcing (i.e. terrain features, temperature contrasts, etc.) than the initial conditions. Limited knowledge of the kind of instability present in the equatorial regions makes it difficult to initialize these meso-scale numerical models.

In order to study the response of changing roughness length on the development of meso-scale flows over Kenya, the wind fields were initialized to zero (i.e. u=v=w=0) at 0500 hours local time. At this time the flow can be assumed calm over Kenya, and in the months of April and May the flow along the coast is generally southerly with little influence of synoptic-scale flow into the interior of the domain as suggested by Okeyo (1982) . Since the integration starts with an atmosphere at rest, we assume that the treatment of initial conditions may not influence strongly the outcome of these simulations.

The initial conditions for temperature and humidity fields were taken from radiosonde sounding typical of May from

/Tot- 4° 04',
„ 52') and Garissa (Lat.
Mirobi (Ut. I' 16'. [36] " }
aCCordin g to
These data were initialized
39- 41'). These equat orial regions
•t al (1978). Over Kenya, and the q
Warner it ai- /
due
. eneral upper air data posses a big problem,
in general, uppe Since we
t0 unavailability of adequate upper air statins.

dealing wit. the development of **meso**-scale flows and
t M **large**-scale flows over the domain of study, the initialized data give a good representative for this study.

2.7.2 BOUNDARY CONDITIONS

Specification of meteorological variables at boundaries is a fundamental problem when using Limited Area Models **(LAM's)**. In General Circulation Models (GCM's), lateral boundary conditions are eliminated by considering the entire global domain. Treatment of boundary conditions varies from one atmospheric phenomenon to another. The solution in the interior of the domain is sensitive to variations in the boundary conditions. Generally, the lateral boundary conditions are located far enough from the region of interest - that the errors induced at the boundaries remain within
Bomeacc* Pfbl« tolerance in the interior of the do •
• e oomam during
forecast period.

There are five types of boundary conditio
^is model; (1) fixed * Condltlo»s Possible in
J lxed,
time dependent
""low/outflow-dependent (SW), (4) spon ' "
' 1 ' Pongе (Perkey and

Kreitzberg 1976), and (5) Relaxation (Davies and Turner 1977).

Fixed boundary condition is the simplest where all the prognostic variables at the boundaries are specified initially and remain constant with time. These boundary conditions are useful for some theoretical studies. This and the other time dependent boundary conditions have been discussed extensively by Anthes et al. 1987.

In this study we use the lateral boundary conditions which consist of large-scale time-varying tendencies linearly combined with model calculated tendencies. The large-scale tendencies for temperature and specific humidity are from real data analysis of these variables, while large-scale tendencies of velocity components are assumed to be zero. This type of boundary condition is referred to as 'sponge' condition by Perkey and Kreitzberg (1976).

The sponge boundary condition is given as:

(46)

where n-1,2,3,4, for cross-point variables

n=l,2,3,4,5, for dot-point variables.

a represents the variable, the subscript MC denotes the model calculated tendency, and LS the large-scale tendency, which is obtained either from observations or large-scale model simulations, and n is the number of grid points from the

nearest boundary (n=1 at the boundary). The weighting coefficients w(n) for cross-point variables from the boundary inward are 0.0, 0.4, 0.7, 0.9, while for dot-points variables are 0.0, 0.2, 0.55, 0.8, 0.95. All other interior points have w(n)=1.

The next section presents the details of the numerical experiments which were performed in this study.

2.8 NUMERICAL EXPERIMENTS

Three numerical experiments were performed in this study in order to examine the effects of changing roughness on the meso-scale flow and the general weather pattern over Kenya. Integrations were started from rest while the land surface temperature was calculated from the heat budget equation. The experiments included the model test experiment together with the use of homogeneous and heterogeneous roughness terrain surfaces over the domain of study respectively, as discussed below.

1. THE MODEL TEST EXPERIMENT

The first experiment was taken as a model test experiment. We utilized data for the roughness length over land as a constant as in Okeyo (1987). The experiment was carried out in order to test how well the model could simulate the meso-scale circulations over Kenya.

2. CHANGE IN ROUGHNESS LENGTH OVER A HOMOGENEOUS TERRAIN

The second experiment was performed to determine the effects of changing roughness length on the meso-scale flow over Kenya. Roughness length values of 15 cm, 110 cm, and 10 cm were used in the experiment to represent savannah grasslands, urban, and desert surfaces respectively. The values of surface roughness and other land surface parameters (albedo, moisture availability, etc.) were taken as homogeneous everywhere over land.

These experiments were performed assuming the land surface was initially Savannah with z_0 = 15 cm. Forestation and urbanization was then introduced by increasing z_c to 110 cm. A roughness value of 10 cm was used to represent the effect of desertification due to man-made modification of natural vegetation such as overgrazing, burning, over cultivation, etc.

3. CHANGE IN ROUGHNESS LENGTH OVER A HETEROGENEOUS TERRAIN

In the final experiment roughness values for heterogeneous terrain were used. Initialization of roughness at each grid point of the domain based, on the terrain, vegetation, and land use characteristics of Kenya was made. The indices of the roughness values used in this study were based on table 1 by Weiringa (1986) for the vegetation and urbanization, and Fiedler and Panofsky (1972) for the

geomorphological features.

Results obtained here were compared with the day's and observed mean features over Kenya. In the next chapter we discuss the results obtained from these numerical experiments.

TRBLE 3.0: Specified constants in the primitive equations model used in the experiments (Okeyo 1987).

Parameter	Numerical value	Remarks
P,	100 hPa	pressure at the top of the model
	0.1 for u,v,t,q_v,p*	smoothing coefficient in the time filter domain
f	o s^1	coriolis parameter
$K_{H}o$	$4x10^4$ mV	constant horizontal diffusion
κ	0.35	Von-karman constant
At	120 sec.	time step
1	**100 m.**	mixing length
Rk	**1.0**	critical Richardson number
Rzo	1 $m^2s"'$	constant critical diffusion
q«,	$5x10^4$ $kgkg^1$	critical value for onset auto-conversion
K,	$10"^3$ s'^1	
Ax	$l.lllxlO^3$ m.	grid length
A	**0.2**	surface albedo over land
	0. 06	surface albedo over water
M	**1.0**	moisture availability over water
	0.1	moisture availability over land
	0.02 cm.	surface roughness over water
	varied	surface roughness over land

CHAPTER 3

3.0 RESULTS AND DISCUSSION

Numerical experiments were performed to study the effect of changing roughness length on the meso-scale flow over Kenya. The first experiment highlighted the response of the model to the diurnal forcing over Kenya. In the second experiment surface roughness values were varied homogeneously over the domain and the effects on meso-scale flow examined. The final experiment took into consideration specification of roughness values at each grid point of the domain. These experiments were designed with reference to the geographical and physical features of Kenya, and the equatorial atmosphere, but can be applied in any region with some modifications.

At the start of the integrations, the atmosphere was assumed to be at rest. The land surface temperature was calculated using the heat budget equation. The parameters used are given in table 3.0. The results obtained from these experiments are discussed in the following subsections.

3.1.0 THE MODEL TEST EXPERIMENT

Meso-scale flow systems have a horizontal scale of the order of a few kilometers, to a few hundred kilometers, with a time scale of one hour to one day. The vertical scale extends from tens of meters to the depth of the troposphere (Okeyo 1987).

In order to determine the response of the model to the meso-scale flow over Kenya, the analyses were performed at 0600 hours and 1800 hours local time. The observed horizontal and vertical motion fields are presented independently in the next sections.

3.1.1 THE HORIZONTAL MOTION FIELDS

The flow pattern of zonal wind component (u), at 0.5°S across Kenya at 0600 hours (Figure 8), shows a thin layer of westerlies extending from surface to 950 (hPa) level. This westerly flow occupies most parts of the eastern slopes of the highland areas and the coast. Easterlies overlie the low-level westerlies, in the levels 950 hPa and 750 hPa. The low-level westerly flow constitutes the land-breeze and down slope flow towards the Indian Ocean. This flow is induced by the rapid radiative cooling of land at night, generating the land-ocean pressure gradient with the resulting flow from land to ocean at night and early morning. This meso-scale low-level westerly flow is dominant in the absence of the prevailing easterly flow. The land breeze and down-slope flow in the eastern slopes of the highlands converges, and also decelerates the prevailing easterly flow in this area in the night and early morning to cause condensational cooling which results in light drizzle. Likewise, the flow to the west of the domain shows down-slope and land breeze, easterly flow

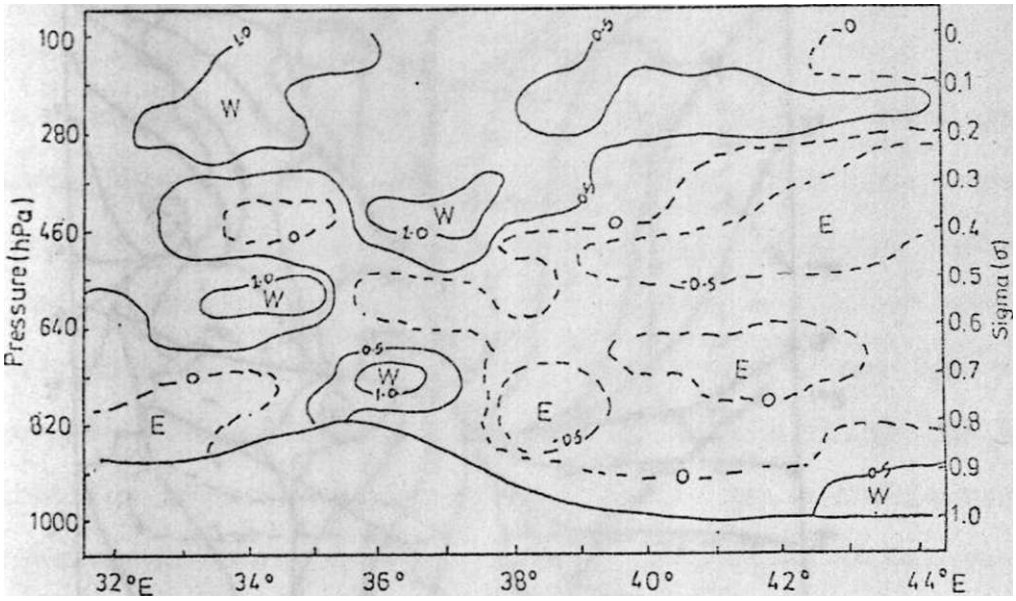

Fig. 8 East-West cross-section of the Zonal wind along lat. C.5°S over Kenya, at 0f:00h Local lime (Isoline interval of 0.5 isi/s). (lil'a - hectol'ascal pressure level).

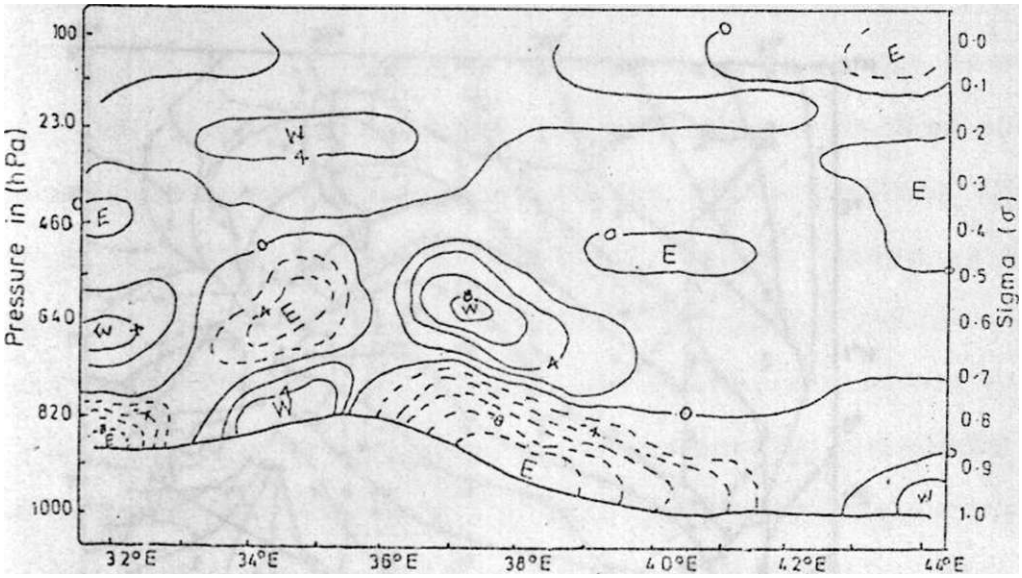

Fig. 9 Fast-West cross-section of the Zona! wind along lat. *0.5'S* over Kenya, at ISOOli Loca! time. (Isoline interval of 2.0 ni/s).

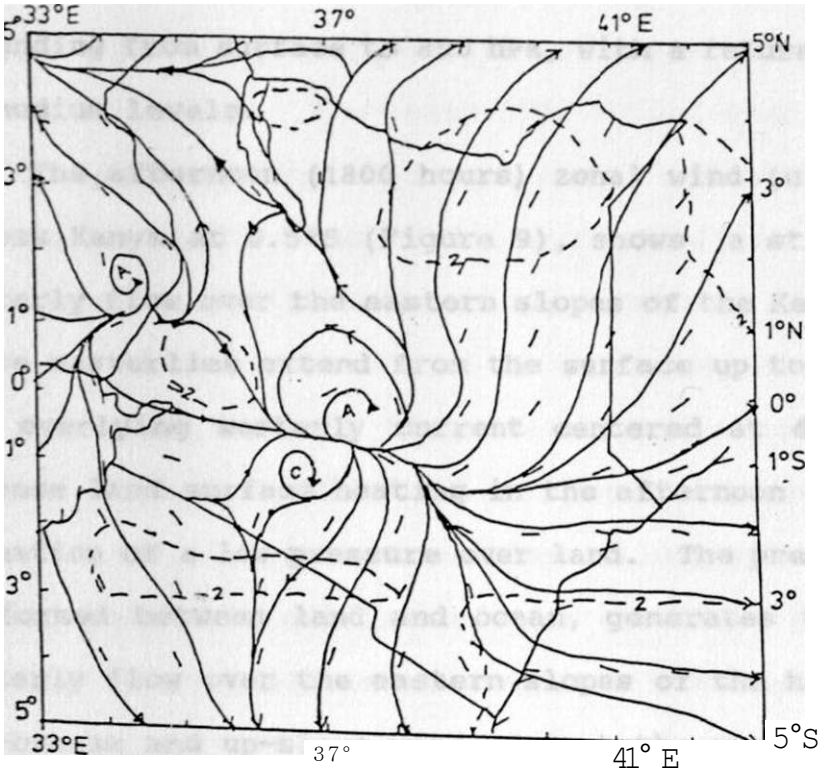

Tig- 10 Streamline and Isotach analysis over Kenya at level «r- 0.95 W1OhPa) for 0600h Local time

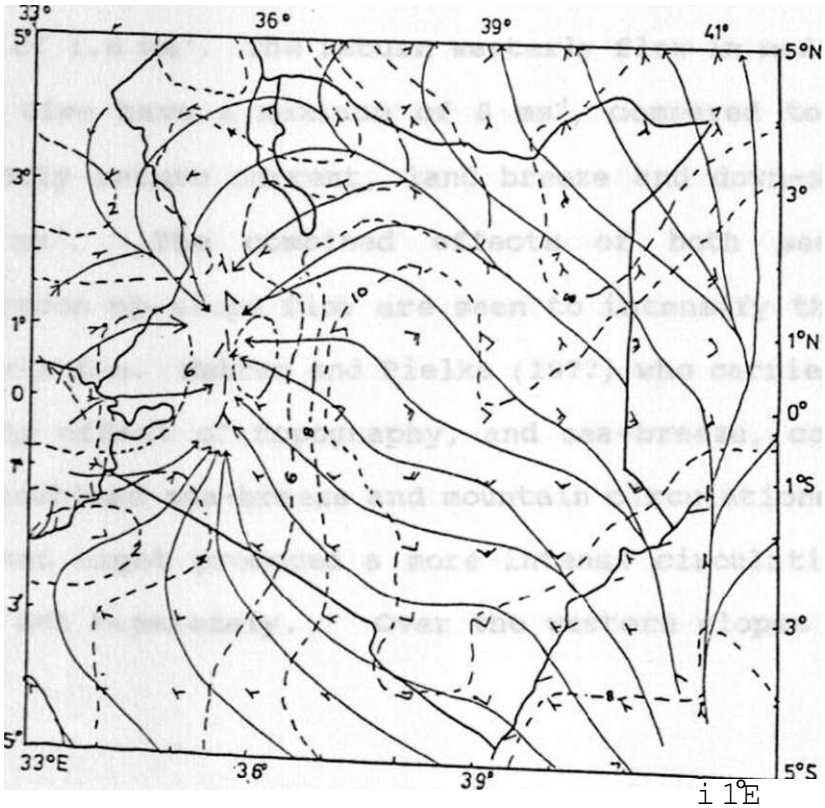

extending from surface to 850 hPa, with a return westerly flow in medium levels.

The afternoon (1800 hours) zonal wind (u) flow pattern across Kenya at 0.5°S (Figure 9), shows a strong low-level easterly flow over the eastern slopes of the Kenya highlands. These easterlies extend from the surface up to 730 hPa, with the overlying westerly current centered at 640 hPa level. Intense land surface heating in the afternoon results in the formation of a low pressure over land. The pressure gradient so formed between land and ocean, generates this low-level easterly flow over the eastern slopes of the highlands. The sea-breeze and up-slope wind augment the prevailing easterly flow, to form strong low-level easterly currents over the eastern highlands. The low-level easterly winds attain a maximum of about 11.1 ms^{-1} as compared to weak morning westerly flow of 1.6 ms^{-1}. The return westerly flow in medium levels at this time have a maximum of 8 ms^{-1}, compared to the morning easterly return current, land breeze and down-slope flow of 0.4 ms^{-1}. The combined effects of both sea-breeze and afternoon up-slope flow are seen to intensify the meso-scale circulation. Mahrer and Pielke (1977) who carried out a study on the effect of topography, and sea-breeze, concluded that the combined sea-breeze and mountain circulations during both day and night produced a more intense circulation than when they act separately. Over the western slopes we observe

low-level westerly current with an overlying easterly flow in the medium levels. The westerlies extend from the surface to 800 hPa level, with the return easterly current centered at 600 hPa level. The westerlies and easterlies have a maximum speed of 5.9 ms"[1] and 5.3 ms"[1] respectively. This afternoon lake-breeze and up-slope flow is in the opposite direction to the prevailing easterly flow. With a coarse resolution of 1°x 1° used here, we were not able to simulate a magnified evolution of the lake and land breeze over the western slopes which have horizontal dimension of less than 100 km.

The morning streamline analysis over Kenya (Figure 10) shows low-level divergent winds from an anticyclonic vortex centered over the western highlands. Low-level winds are generally weak having a maximum speed of 1 ms"[1], over the domain. The divergence of low-level winds in this area is responsible for the clear skies usually observed here at night and early morning. The afternoon streamline analysis (Figure 11) , shows strong easterlies (with a maximum speed of 11 ms"[1]) from the coast towards the highlands. To the west of the highlands we observe winds with a maximum speed of 6 ms[1] from the lake towards the highlands. Convergence between the sea-breeze and up-slope flow from the east and lake-breeze and up-slope flow from the west is located over the western slopes. This convergence results in the formation of deep afternoon clouds which result in showers, hail with accompanying

thunderstorms (Sansom and Gichuiya 1971, Okeyo 1987). Lumb (1970), Asnani and Kinuthia (1979) did some observational studies on the lake-breeze over kenya and concluded that, the lake-breeze over western Kenya interacts with prevailing easterly winds to yield the observed afternoon weather. Okeyo (1987) showed from a numerical study, that the cumulus convection in this area is responsible for supplying latent heat in the meso-scale circulation while the lake breeze and the synoptic-scale flow supplies the moisture and maintains the circulation.

3.1.2 VERTICAL MOTION FIELD

The night time and early morning vertical velocity field (Figure 12), shows a rising motion with a maximum of 4.3 x 10"' cms"[1] over the lake, and sinking motion having a maximum of 14.8 x 10"' cms"[1] to the east of the lake. Rising motion of 18.8x10"' cms"[1], is observed over the high ground area. The maximum upward motion is located at 550 hPa level. Sinking motion of 20.4x10"' cms"' is observed over the entire area to the east of the highlands. The maximum intensity is located at 550 hPa, level. Over the western slopes there is low-level convergence centered over the lake as shown by the upward motion field.

In the afternoon (Figure 13), there is strong vertical motion over the western slopes of the highlands. A maximum

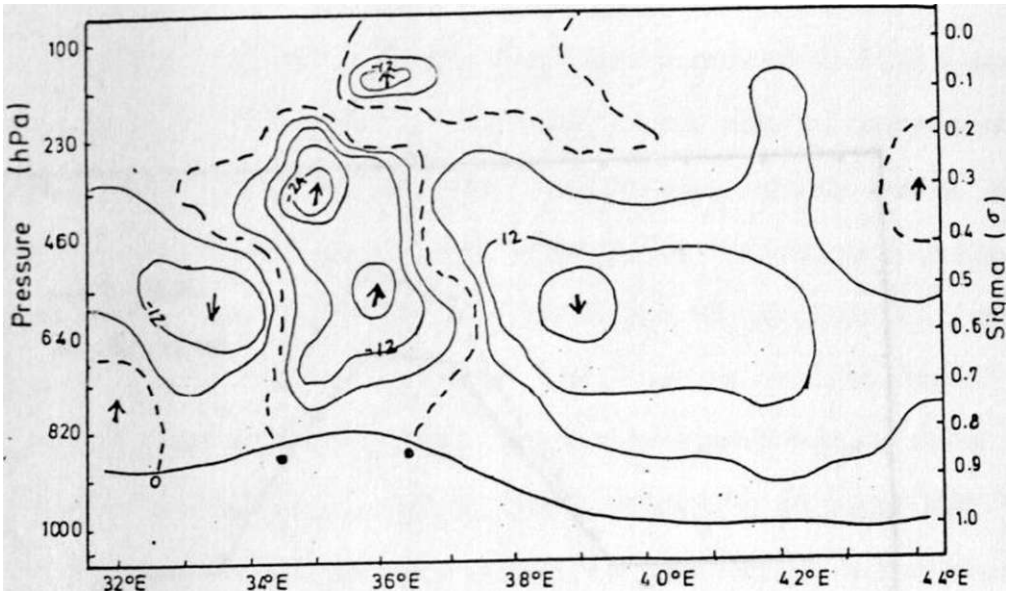

Fig. 12 A cross-section of vertical motion field along lat. 0.5°S over Kenya, at 0600h Local time, (Isoline interval of 6 x 10*1 cm/s).

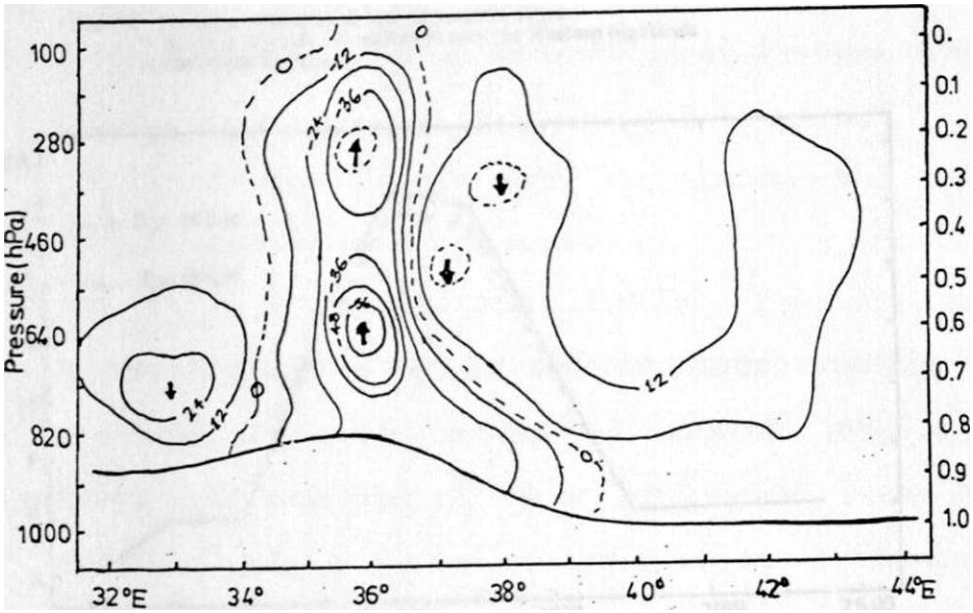

Fig. 13 A cross-section of vertical motion field along lat. 0.5° S over Kenya, at 1800h Local time. (Isoline interval of12x 10^{-1} cm/s).

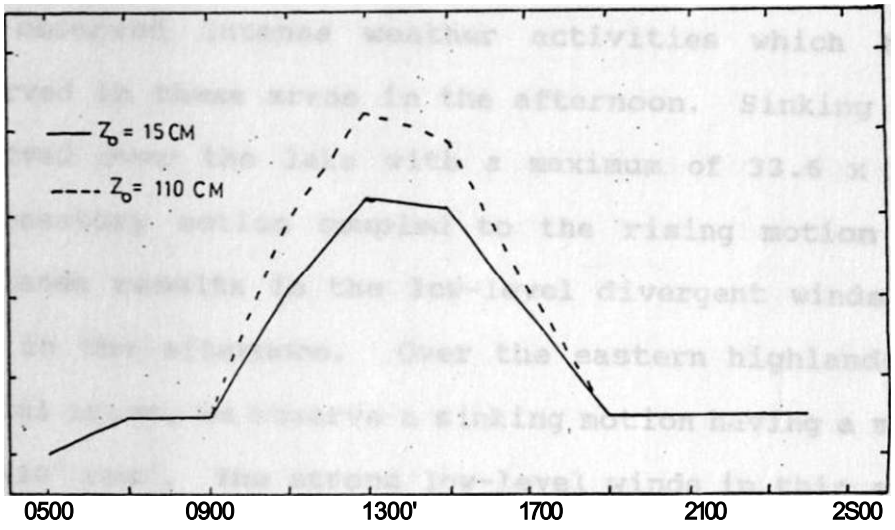

Local time (hours)..

Fig. 14 Temporal variation of the Horizontal stress at level C=0.95 910 hPa) over the Western highlands (Urbanization Case).

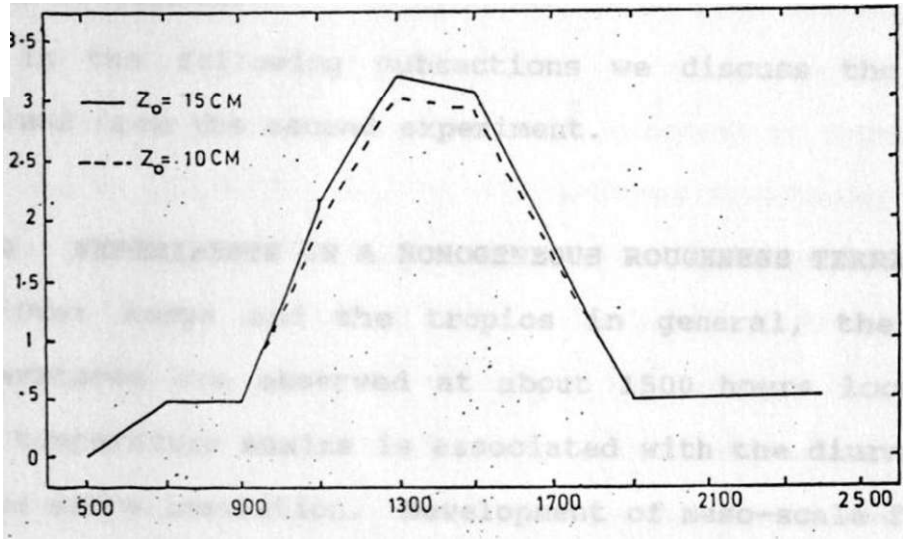

Local time (hours) .

Fig. 15 Temporal variation of the Horizontal stress at level (T=0.95 ("» 010 hPa) over the Western highlands (Desertification Case).

vertical motion of 57.1 x 10"' cms"[1] is observed in this area, centered at 640 hPa level. This vertical motion agrees with the observed intense weather activities which have been observed in these areas in the afternoon. Sinking motion is observed over the lake with a maximum of 33.6 x 10"' cms"[1]. Compensatory motion coupled to the rising motion over the highlands results in the low-level divergent winds from the lake in the afternoon. Over the eastern highlands and the coastal areas, we observe a sinking motion having a maximum of 21.5x10"' cms"[1]. The strong low-level winds in this area cause low-level divergence and thus inhibit upward motion. The sinking motion over these areas and the accompanying low-level diffluence explains the little convective activities observed in the afternoon.

In the following subsections we discuss the results obtained from the second experiment.

3.2.0 EXPERIMENTS ON A HOMOGENEOUS ROUGHNESS TERRAIN

Over Kenya and the tropics in general, the maximum temperatures are observed at about 1500 hours local time. This temperature maxima is associated with the diurnal cycle of the sun's insolation. Development of meso-scale flow over Kenya is dependent on the land and water temperature contrasts, which results from differential solar heating of land and water surfaces. The effect of changing roughness on

the development of meso-scale flow over Kenya was therefore studied at 1500 hours local time. The results are presented in the following subsections.

3.2.1 SURFACE STRESS AND BOUNDARY LAYER WIND SPEED

In this model, surface stress is computed from $r = pu^{*2}$, where p is the air density and u* is friction velocity computed from equation (26) . Thus the surface stress is a function of friction velocity which depends on a surface roughness, z_0. An increase in surface roughness would cause a corresponding increase in surface stress.

Increasing, homogeneously, surface roughness from z_0=15 cm (savannah grassland) to z_c = 110 cm (urban area conditions) results in an increase in surface stress as shown in Figure 14. The temporal variation of surface stress over the western highlands show that this increase is apparent from 0900 hours. From 0900 hours, the induced land/water pressure gradient generates strong winds which are resisted by the surface roughness. An increase of about 0.01 Nm'^{2} in the surface stress is realized at 1500 hours in this case, (about one third). Likewise, a decrease in surface roughness length from savannah to desert conditions (Figure 15), results in a corresponding decrease in surface stress. A decrease in surface stress of about 0.003 Nm^2 (about one twelfth), is realized at 1500 hours local time.

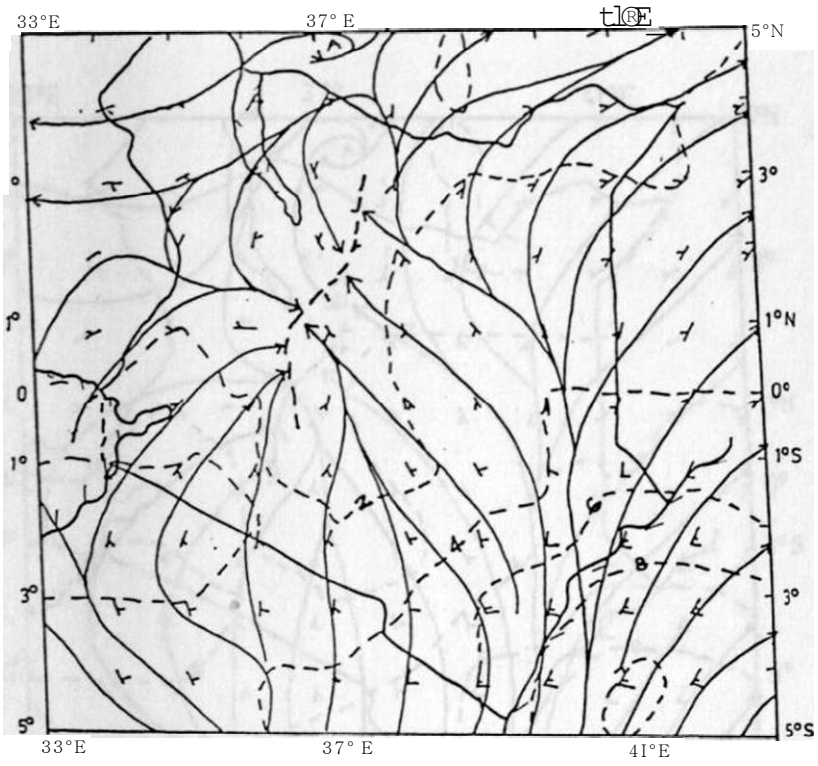

Fig. 16 Streomline and Isotnch analysis over Kenya at level 6=0.95 (910hPa) for z_u =15 cm. (1 full feather represents 5 m/s).

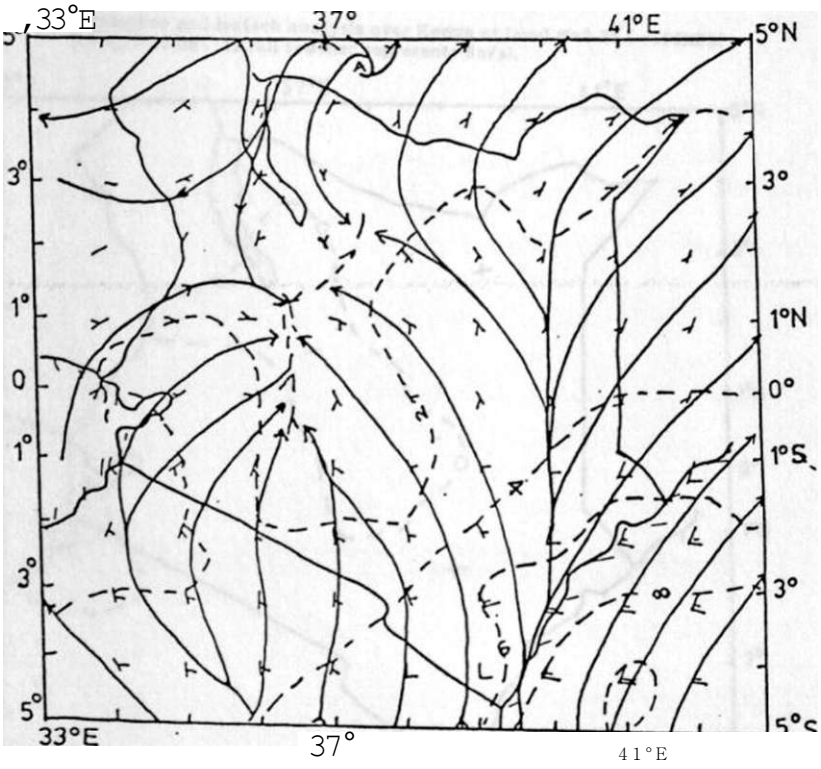

Fie_17 ^i-ora v ^ ^ ^ s 95 <-«««•>

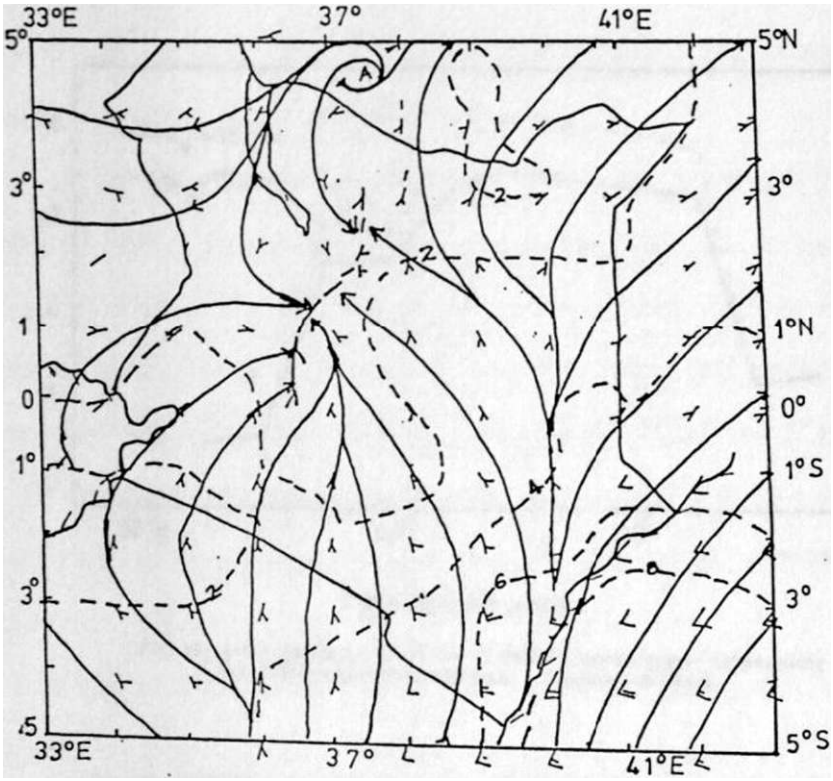

Ki, I. SU0.$_m$nne and . s o u . f f = 0 , 5 (·910hPo)

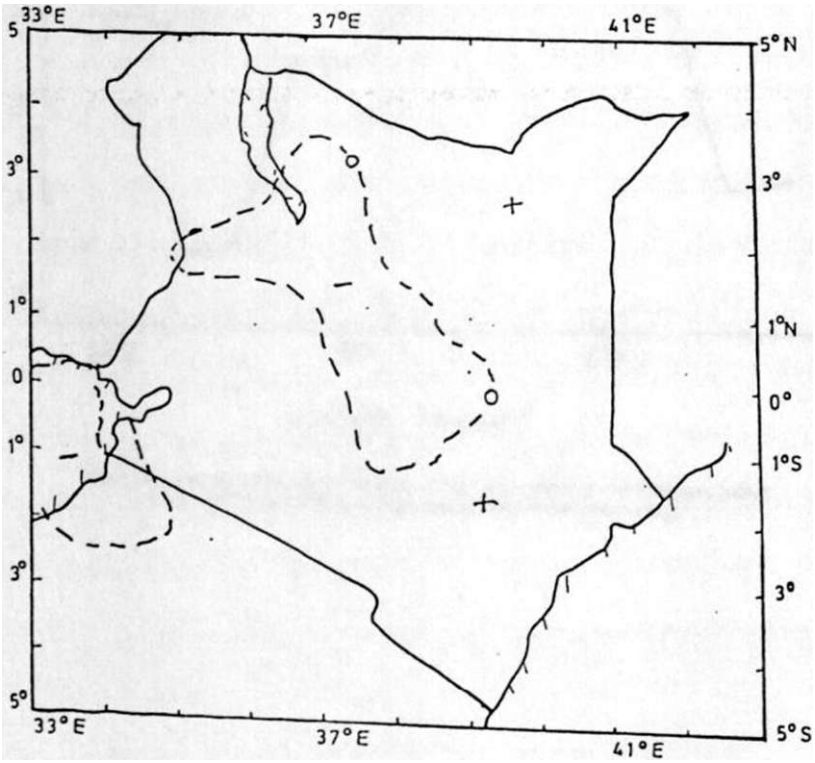

Fig.19 Change in wind speed [speed (z'-=15) - sneoH (t „ , « , 1

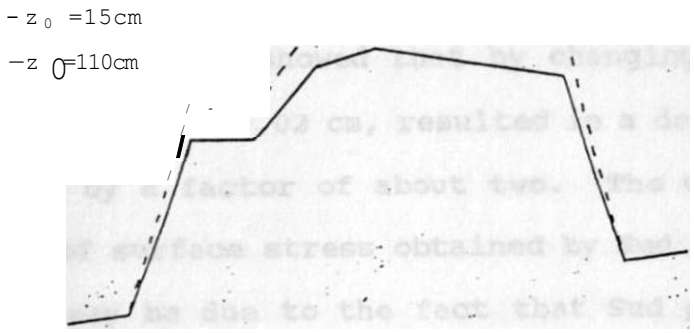

Fig. 20 A horizontal cross-section of Friction velocity over Kenya, along lot. 0.5®S, at ISOOh Local lime. (Urbanization Case).

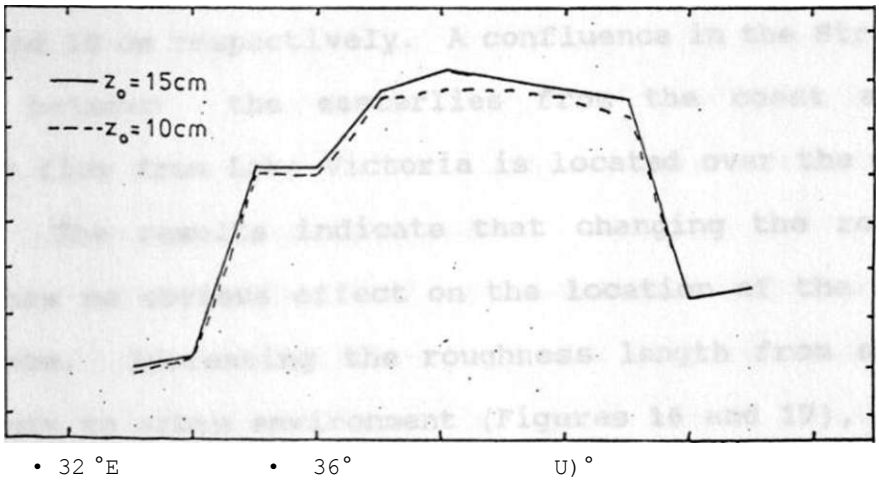

Fig. 21 A horizontal cross-section of Friction velocity over Kenya, along lat. 0.5'S, ot 1500h Local time (Desertification Case).

The results show that changing the surface roughness to urban environment would modify surface characteristics by increasing the surface stress.

Sud et al. (1988), showed that by changing the surface roughness from 45 cm to 0.02 cm, resulted in a decrease in the surface stress by a factor of about two. The difference in the magnitude of surface stress obtained by Sud et al. (1988) and our study may be due to the fact that Sud et al. (1988) used a general circulation model which included large-scale flow. This resulted into stronger surface winds and surface stress.

Figures 16-18 show the streamline analysis over Kenya at 1500 hours local time. The land roughness length is 15 cm, 110 cm and 10 cm respectively. A confluence in the Streamline pattern between the easterlies from the coast and the westerly flow from Lake Victoria is located over the western slopes. The results indicate that changing the roughness length has no obvious effect on the location of the line of confluence. Increasing the roughness length from savannah grasslands to urban environment (Figures 16 and 17), results in a decrease of about 0.5 ms^{-1} (about 25%) in the wind speed. The decrease in wind speed can be explained to be due to the large surface stress generated by high roughness length to the surface wind flow. The surface roughness generates the frictional drag experienced by the surface winds. Over the

area where the steamline pattern converge (Figure 19) a small increase in surface layer wind speed is observed with an increase in surface roughness. Zhang and Anthes (1982), showed that an increase in roughness length, increased the turbulent mixing and hence convergence. An increase in turbulent mixing, increases the pressure fall, probably causing the slight increase in surface layer wind speed near the area where the streamlines converge. The increase in the surface wind speed may also be explained in terms of the downdrafts from the developing cumulus clouds in these convergent areas.

Decreasing the surface roughness from the savannah grasslands to desert conditions (Figures 16 and 18), leads to a corresponding increase in surface layer wind speed of about 0.1 ms^{-1} (about 5%). The small increase in surface wind speed is due to the decrease in the surface stress resulting from the decrease in surface roughness.

These results show that human-induced modification of surface roughness by urbanization would increase the surface stress and hence reduce the wind speed within the boundary layer. Likewise, human activities such as deforestation and overgrazing, that lead to desert-like conditions would increase the boundary layer wind speed in the region. The general impact of changing surface roughness over Kenya is to modify the meso-scale wind speed, and hence change the

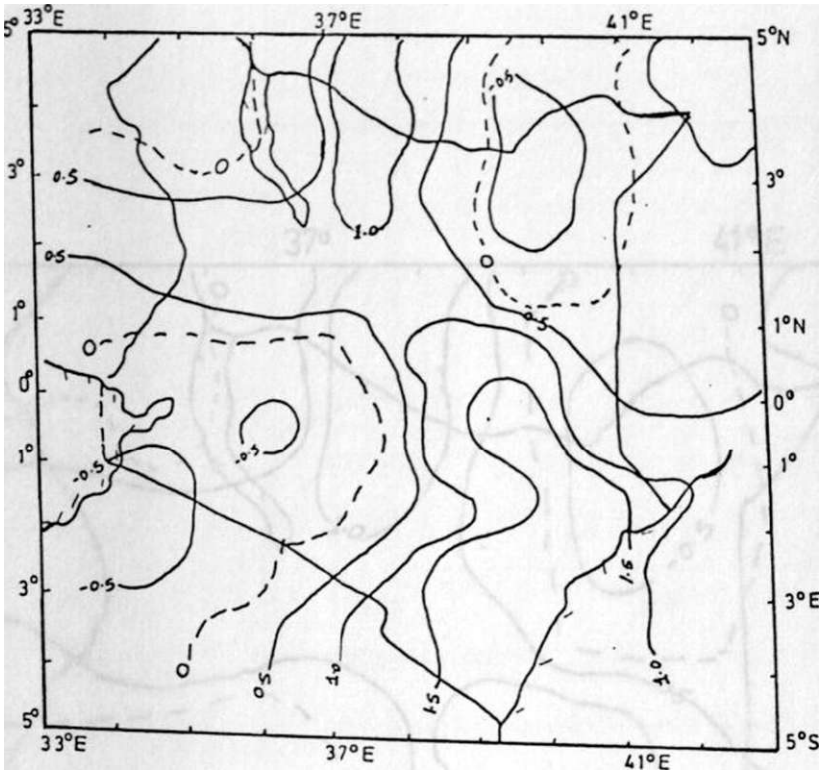

Fig. 22 The divergence field over Kenya at level r=0.9S (-9101,Pa), and 7.0-15cm. (Isolinc interval of 0.5 x 10^{-5} s^{-1})

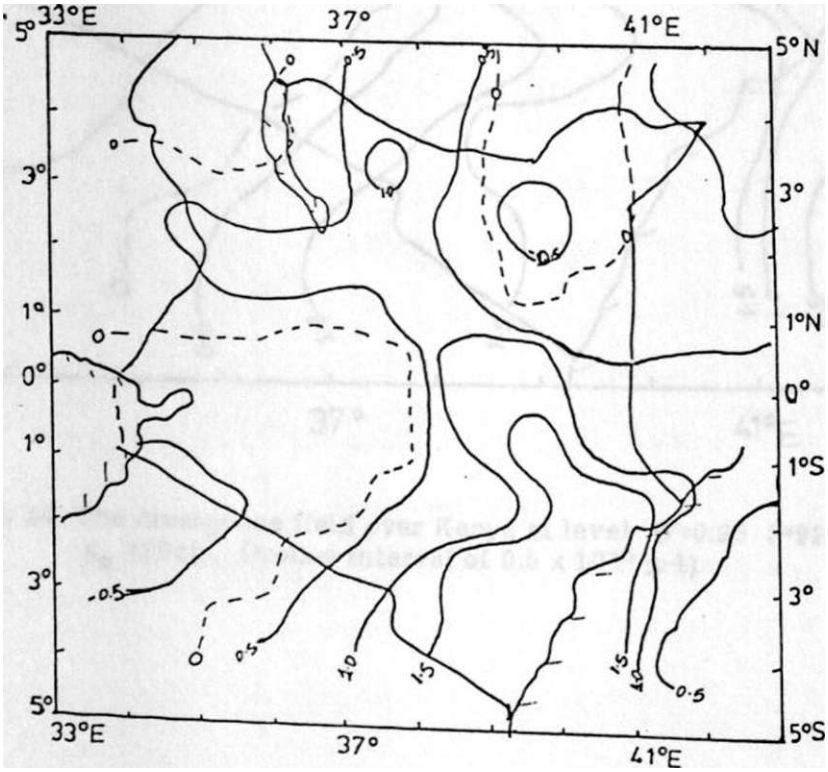

F'g. 23 The divergence field over Kenya at level <r=o 95 f-q, Kkd , , -llOfcW. (Isolinc interval Of 0.5 X 10"5 g-jj (*910hP..), and

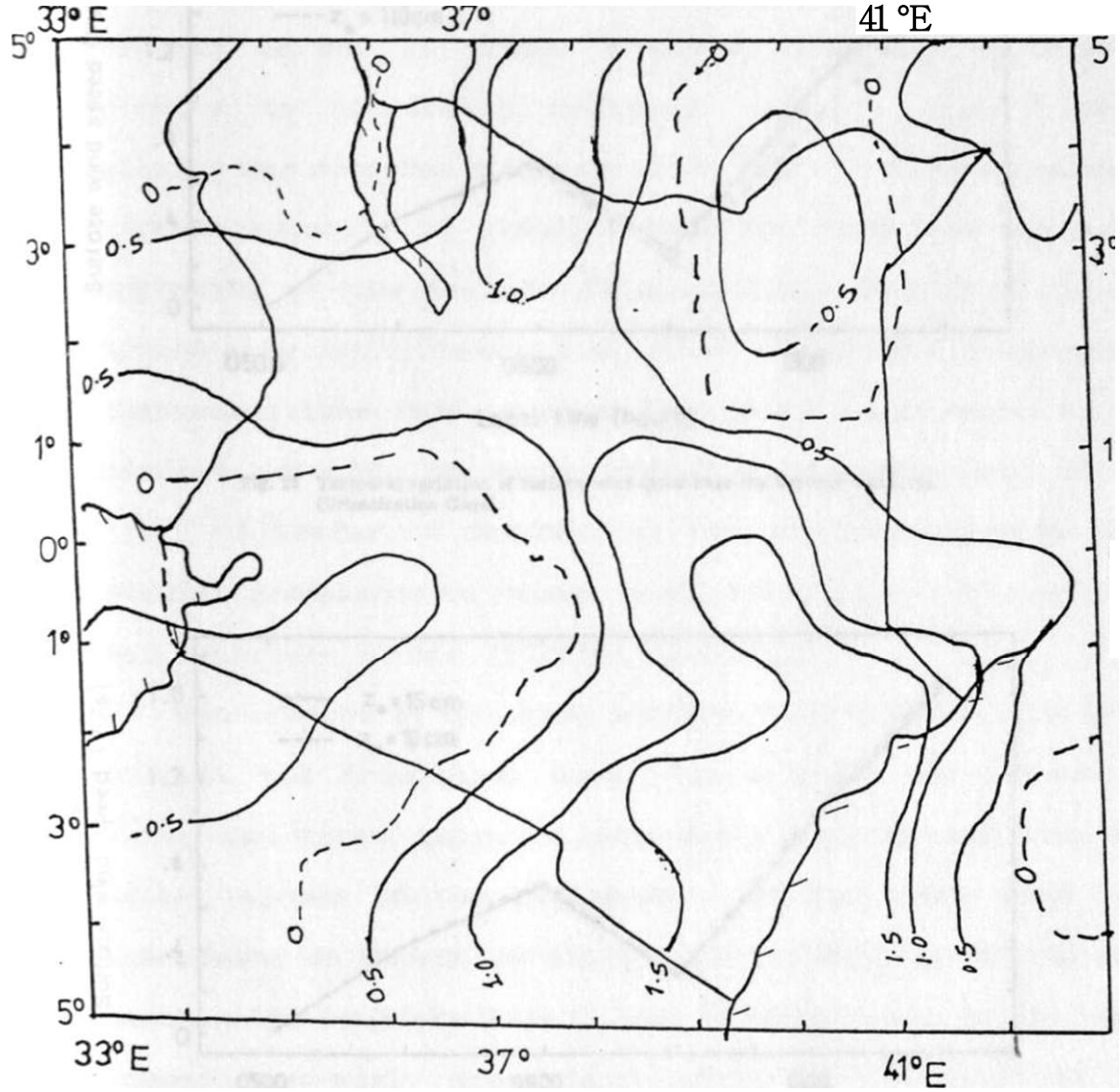

Fig. 24 The divergence field over Kenya at level (T=0.95 (-910hPa), and z_0 =10cm. (Isoline interval of 0.5 x 10^{-5} s-1)

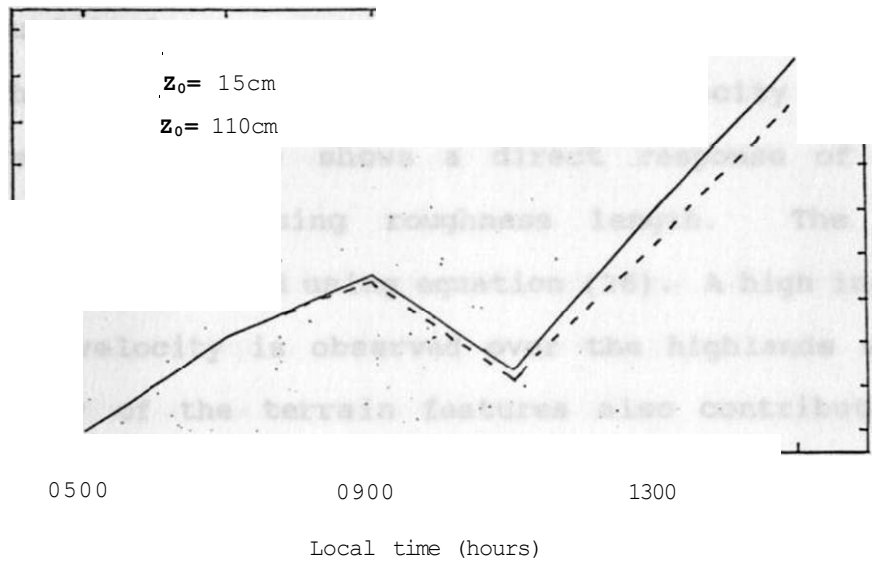

Fig. 25 Temporal variation of surface wind speed over the Western highlands. (Urbanization Case).

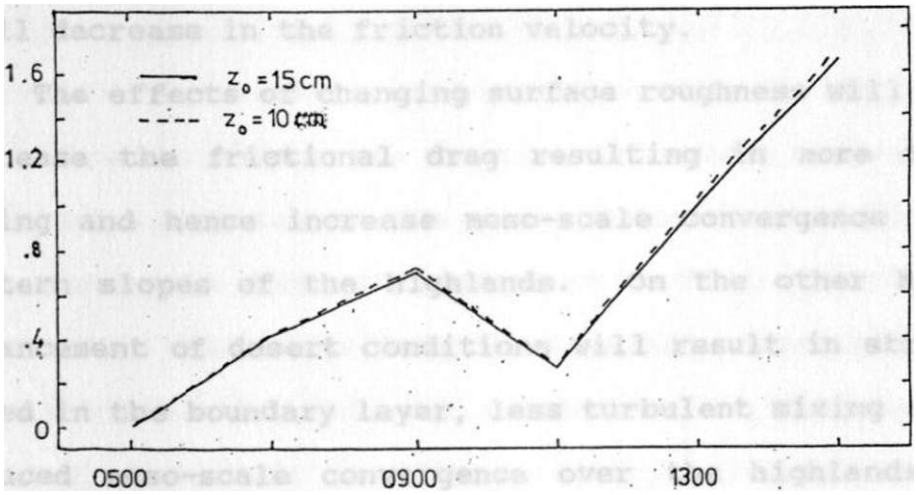

Fig. 26 Temporal variation of surface wind speed over the Western highlands (Desertification Case).

transport of pollutants, dust particles, heat, moisture, in the boundary layer.

The cross-section of friction velocity over Kenya (Figures 20 and 21) shows a direct response of friction velocity to increasing roughness length. The friction velocity was computed using eguation (26). A high increase in friction velocity is observed over the highlands where the complexity of the terrain features also contribute to the surface drag coefficient. Increasing the surface roughness to urban conditions from savannah results in an increase in the friction velocity of about 29% over the highlands (about 37°E). Likewise, a decrease of the surface roughness from savannah grasslands to desert conditions (Figure 21), shows a small decrease in the friction velocity.

The effects of changing surface roughness will be to increase the frictional drag resulting in more turbulent mixing and hence increase meso-scale convergence over the western slopes of the highlands. On the other hand, the enhancement of desert conditions will result in strong wind speed in the boundary layer, less turbulent mixing and hence reduced meso-scale convergence over the highlands in the afternoon.

3.2.2 THE HORIZONTAL DIVERGENCE FIELD

The divergence field was computed from the equation:

$$D = du/Bx + dv/dy \qquad (47)$$

The solution to this equation was made using the centered difference technique. The divergence fields are generally used to infer areas of upward motion where there is low level convergence, and descending motion where there is low level divergence. The divergence fields (Figures 22-24) at 1500 hours local time, show marked diffluence over the eastern sector of the country and the coastal areas. The observed strong winds in this areas, are responsible for the low-level divergence resulting in clear skies as usually observed in the afternoon. Convergence is observed over the western slopes of the highlands. These are the areas of strong meso-scale flow convergence over Kenya. The observed convective activities in these areas in the afternoon result from the convergence between the westerlies from the lake and easterlies from the Indian Ocean. An increase of the surface roughness from savannah grasslands to urban conditions (Figures 22 and 23) results in a decrease of low-level divergence over the eastern highlands of about 0.2 x 10 $"^{5}$ s^{1} (about two-seventh). Likewise decreasing the roughness length from savannah grasslands to desert conditions (Figures 22 and 24), results

in an increase in the low-level divergence over the eastern highlands of about 0.005 x 10^{-5} s^{-1} (about one-tenth) . Over the western highlands an increase in roughness length results in a small decrease in low-level convergence of about 0.04 x 10^{-5} s^{-1} (about one-eighteenth) . Figures 25 and 26 show a reduction in surface wind speed as the roughness is increased and vice versa.

These results show that the roughness length in itself does not play a significant role in the meso-scale convergence over the western highlands of Kenya, but it contributes to the meso-scale convergence by enhancing turbulence mixing of heat and moisture.

The above results have shown that increasing surface roughness from savannah grasslands to urban area conditions modifies the meso-scale flow pattern in the boundary layer. Increasing the surface roughness length increases the frictional drag on the surface wind. This is due to the increase in the boundary layer surface stress. The results show that changes in the surface roughness have the potential of modifying the low-level wind speed and divergence fields in the region. High surface roughness leads to reduced divergence fields over the eastern highlands of Kenya and vice versa. The results have also shown that the surface roughness plays a significant role in the meso-scale convergence over the western slopes of Kenya, by contributing to the turbulent

mixing of heat in the meso-scale circulation.

3.2.3 HUMIDITY, WATER VAPOUR CONVERGENCE AND RAINFALL

The moisture field and water vapour convergence associated with meso-scale circulation over Kenya are important in the development of convection over the western slopes. The main sources of moisture in the region are lake Victoria and the Indian Ocean. The convergence zone over the western slopes is enhanced by the pressure gradient generated between land and water by solar heating and the complex terrain (Okeyo 1982,1987). The spatial distribution of the moisture field across the country (Figures 27-29) at 1500 hours, shows an accumulation of moisture over the western slopes in the afternoon. Relative humidity values of about 99% are observed in the areas of convergence over the highlands. Values of about 68% are observed in the North-Eastern areas of Kenya which are generally dry and arid.

Increasing the surface roughness length from 15 cm to 110 cm results in a decrease of the surface layer moisture of about 2% over the highlands. Over the Northeastern areas of Kenya the decrease is about 4%. A reduction of surface wind speed in the boundary layer as a consequence of increasing surface roughness length results in a reduction of advected moisture to the highland areas. Likewise an increase of about 1% in relative humidity was observed over the highlands

(Figure 29), when surface roughness was reduced from savannah grasslands to desert conditions. This is reflected in a slight increase in surface layer wind speed in this case, resulting in an increase in advected moisture.

The temporal variation of surface specific humidity over the western slopes, (Figure 30) shows a corresponding increase in humidity with an increase in the surface roughness. An increase of about 1% is realized when the roughness length is increased to urban conditions from savannah grasslands. Specific humidity is highest in the late afternoon (from 1800 hours local time). This is due to the contribution from the maximum moisture convergence and precipitating cumulus clouds at this time.

The effect of reducing roughness from savannah to desert conditions (Figure 31), yields a small decrease (of about 0.2%) in the temporal variation of surface layer specific humidity over the western slopes, at 1500 hours local time.

An increase in the surface roughness to urban conditons results in increased turbulent mixing of heat and moisture in the boundary layer. This turbulent mixing could explain the increase in specific humidity over the western highlands of Kenya. Deserts are generally smooth with little turbulent mixing and hence lower specific humidity as shown in Figure 31. These results agree with those of Zhang and Anthes (1982), who showed by using a one dimensional PBL model that

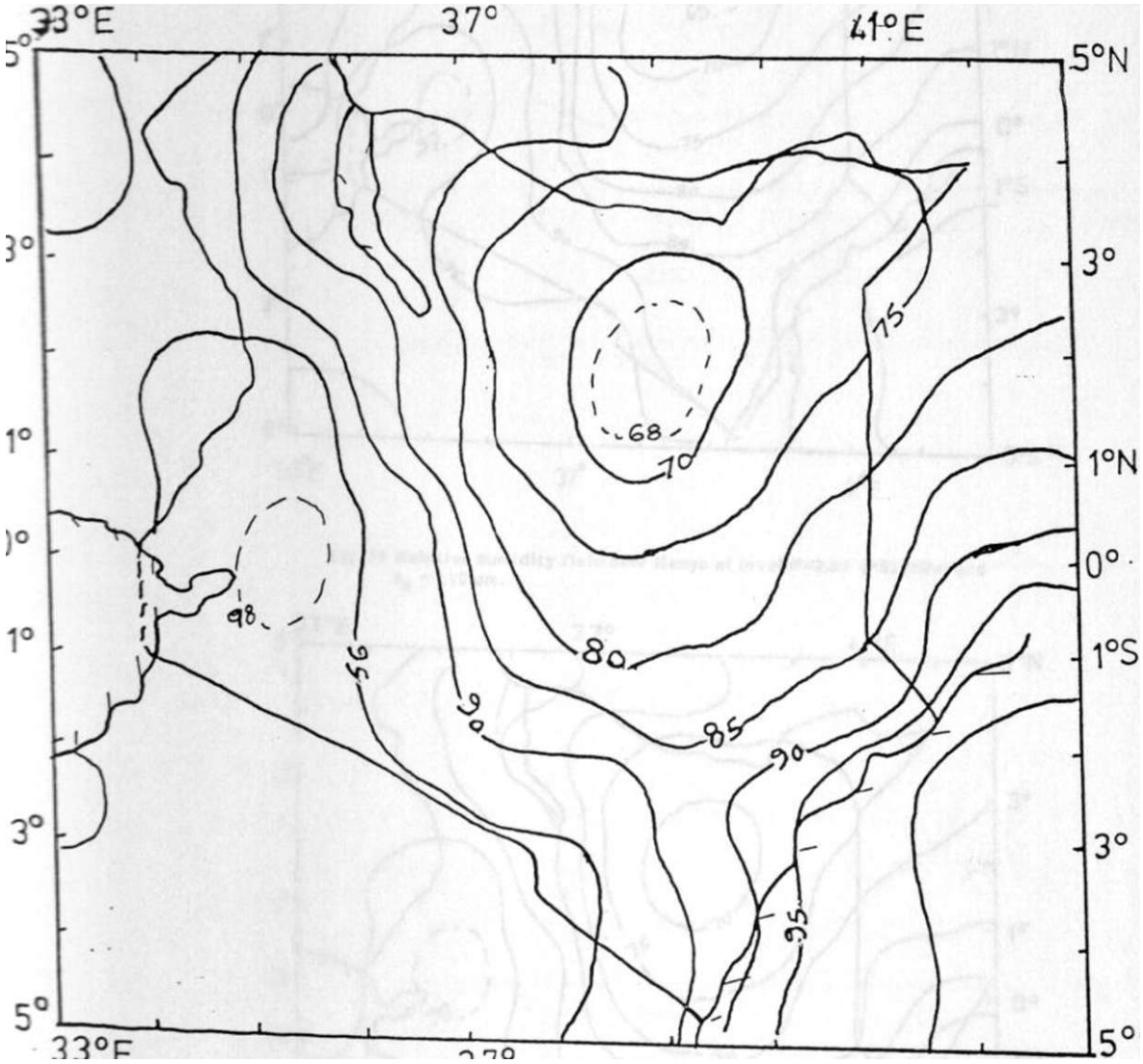

Fig. 27 Relative humidity field over Kenya at level cr=$_0$.95 (^910hPa) and z_0 -15 cmjGsoline interval of 5%).

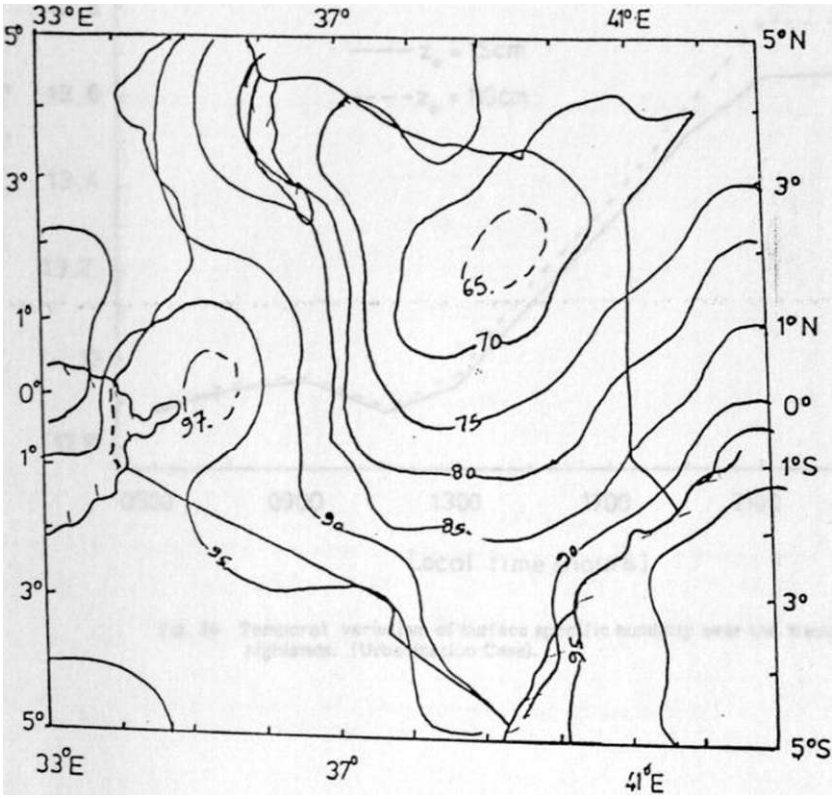

Fig. 28 Relative humidity field over Kenya at level <r=0.35 <"910hPa) and 7- - 110 cm.

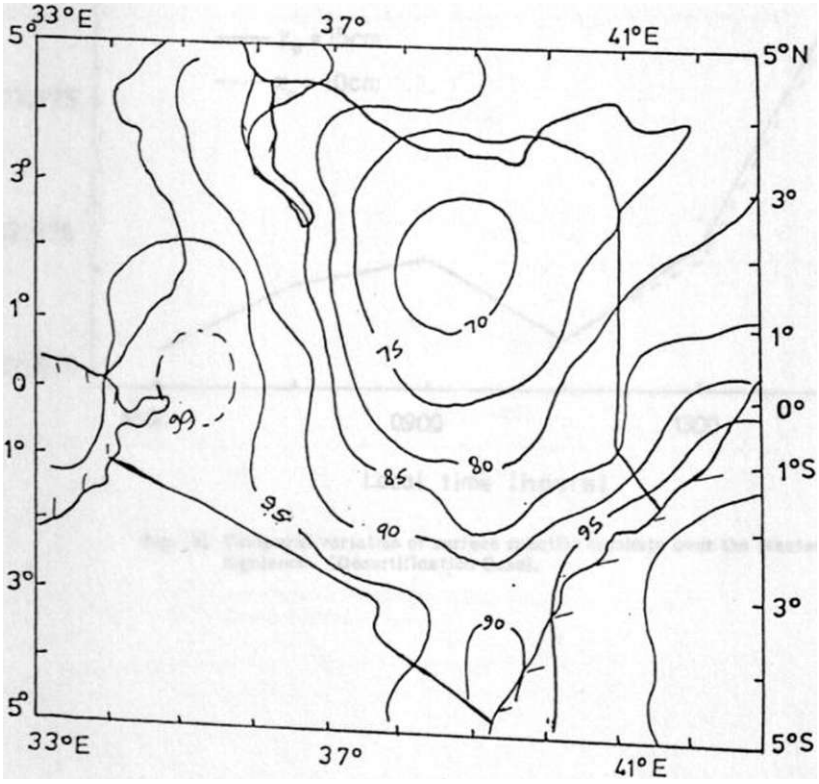

Relative humidity field over kenya at level =o,s, 910hPa)and

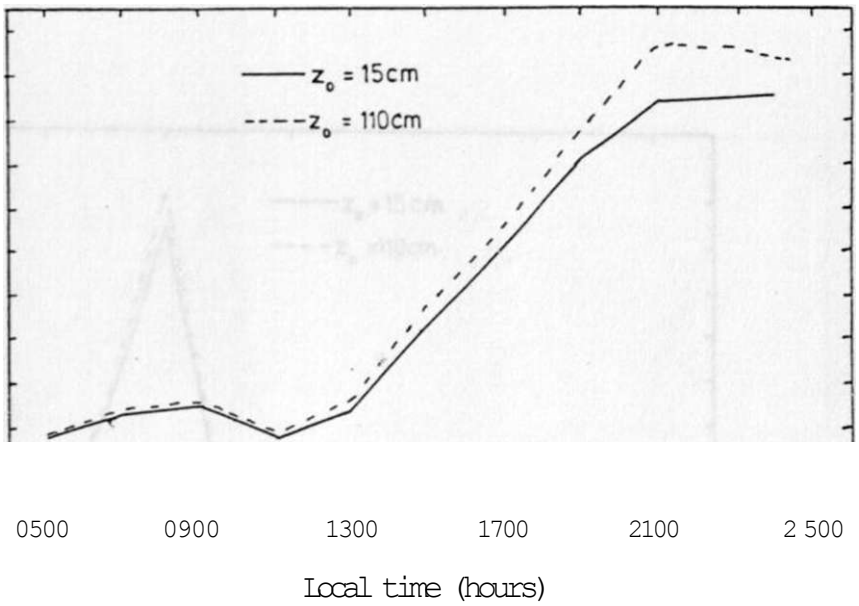

Fig. 30 Temporal variation of surface specific humidity over the Western highlands. (Urbanization Case).

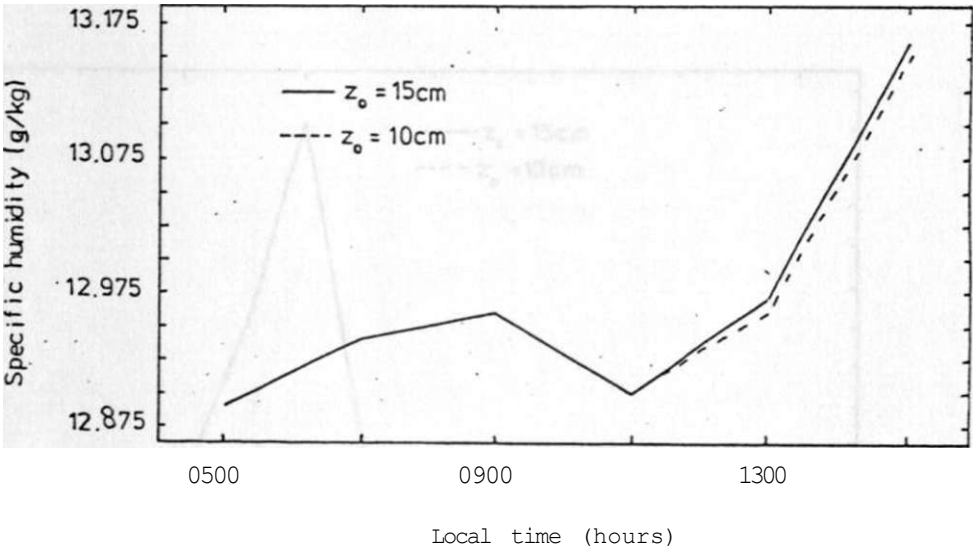

Fig. 31 Temporal variation of surface specific humidity over the Western highlands. (Desertification Case),

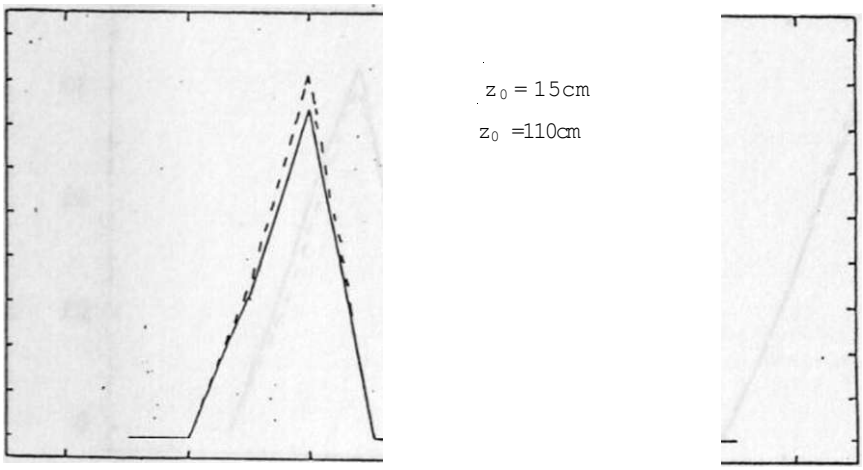

Fig. 32 A horizontal cross-section of a lOh accumulated convectiva Rainfall along lat. 0.5°S. (Urbanization Case).

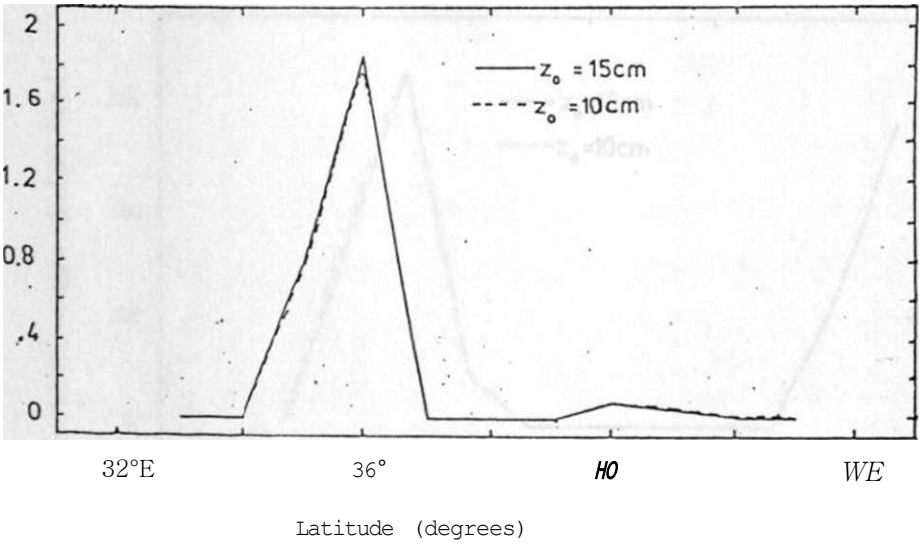

Fig. 33 A horizontal cross-section of a 10H accumulated convective RainfaU along lot. 0.5°S (Desertification Case).

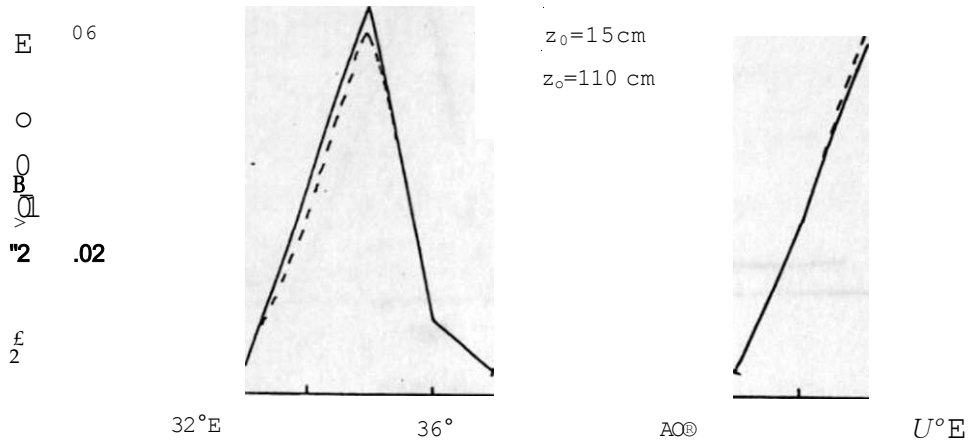

Fig. 34 A horizontal cross-section of a 1 Oh aceumi/latid non-conveietiVe-Rainfall along lat. 0.5°S (Urbanization Case).

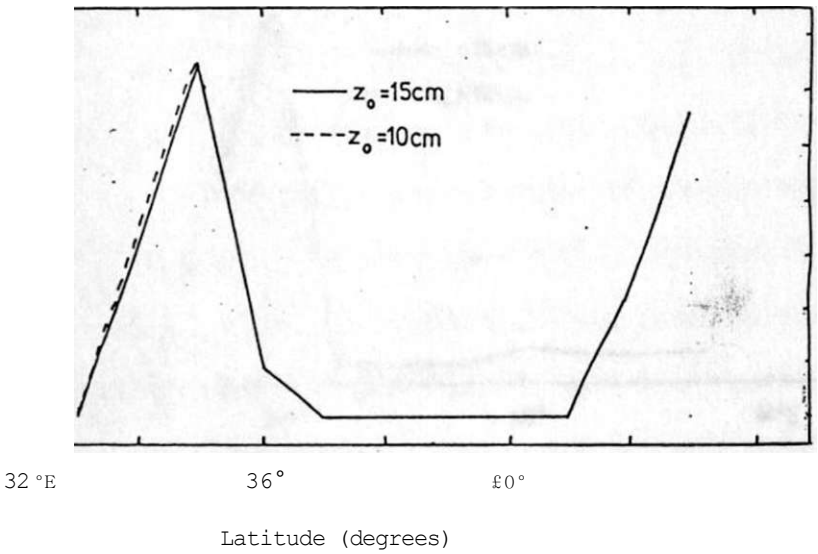

Fig. 35 A horizontal cross-section of a 1 Oh accumulated non-convection Itainfall along lat. 0.5*S (Dcscrtification Case).

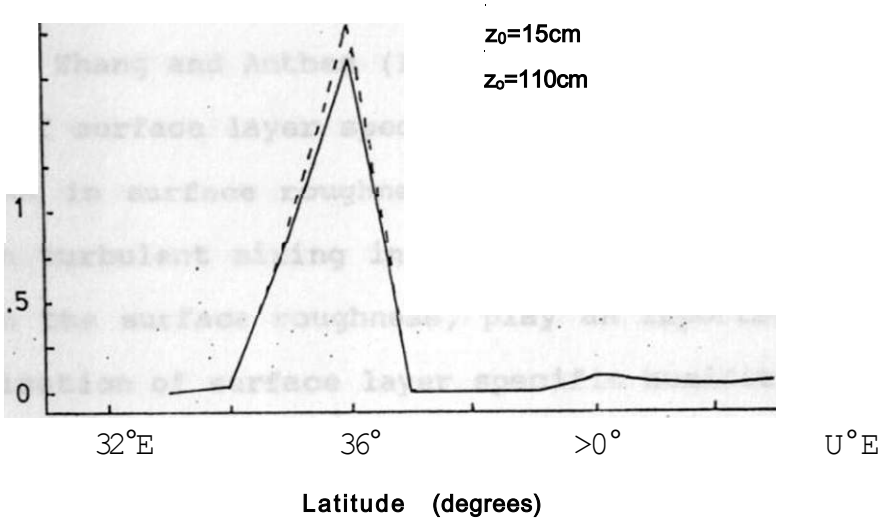

Fig. 36 A horizontal cross-section of a lOh accumulated Total Rainfall along lot. 0.5°S (Urbanization Osc).

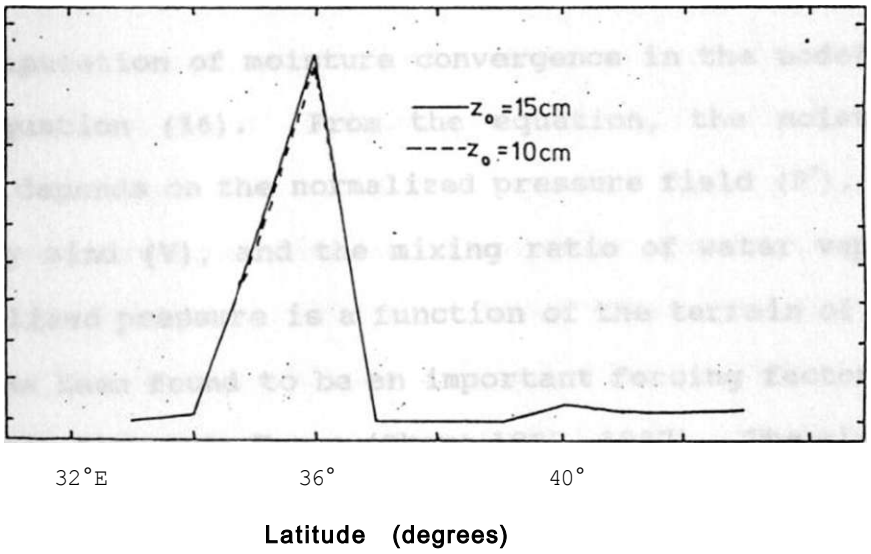

Fig. 37 A horizontal cross-section of a lOh accumulated Total Rainfall along lot. 0.5»S (Desertification Cose).

surface layer specific humidity was sensitive to the surface roughness. Zhang and Anthes (1982) showed that the temporal variation of surface layer specific humidity, increased with an increase in surface roughness. These results show that changes in turbulent mixing in the boundary layer caused by changes in the surface roughness, play an important role in the modification of surface layer specific humidity over the western slopes of Kenya.

The cross-section of a 10-hour accumulated convective rainfall over Kenya (Figures 32 and 33), shows a maximum over the western slopes. In this area deep convective developments are observed in the afternoon resulting in thunderstorms, hail and accompanied showers (Majugu 1983, Asnani and Kinuthia 1979).

The computation of moisture convergence in the model is given in equation (16). From the equation, the moisture convergence depends on the normalized pressure field (P*), the advection by wind (V), and the mixing ratio of water vapour (q_v). Normalized pressure is a function of the terrain of the area, and has been found to be an important forcing factor in the meso-scale flow over Kenya (Okeyo 1982, 1987). The mixing ratio of water vapour in a given area depends on the moisture advected in the area and the local moisture source, which itself depends on the amount of turbulent mixing. An increase in surface roughness has been shown to reduce the surface

layer wind speed and hence slightly decrease the advected moisture in the convergence area. On the other hand turbulent mixing in surface layer increases the specific humidity in the convergence areas of the western slopes of Kenya.

An increase in surface roughness from savannah grasslands to urban area conditions, results in a slight increase in convective rainfall over the western highlands of Kenya (Figure 32). There is an increase in accumulated convective rainfall of about 0.25 mm (about 14%) over a 10 hour period. Likewise a small decrease in accumulated convective rainfall was realized when surface roughness was reduced from savannah to desert conditions (Figure 33) . The effects of a reduction in moisture advection on convective rainfall tend to counteract those of increasing turbulent mixing in the surface layer. Hence the overall effect of changing roughness length on convective rainfall will depend on which one of the two mechanism dominates.

The non-convective rainfall (Figures 34 and 35), shows two peaks of rainfall at 1500 hours local time. One peak is observed over the western slopes and the other at the coast. These rainfall patterns can be explained by the advection of moisture from the lake in the west and from ocean in the east. In this case, low-level wind speed is the important transport agent of moisture contributing to this rainfall. An increase in surface roughness from savannah grassland to urban area

conditions (Figure 34), results in a slight reduction in non-convective rainfall of about 0.03% over a 10 hour period over the western slopes. Little change is observed over the coast. Reducing surface roughness length from savannah grasslands to desert conditions, results in little response in the non-convective rainfall. There is little change in the non-convective rainfall corresponding to small changes in the surface wind speed. The result show that non-convective rainfall play a small role in determining the rainfall field in meso-scale flow over Kenya.

Figures 36 and 37 show that the total 10 hour accumulated rainfall increases with increasing surface roughness. Convective rainfall is the major contributor to this total rainfall.

These results show that the effects of increasing the roughness length results in an increase in the turbulent mixing of moisture in the convergent area of the meso-scale flow over Kenya. Turbulent mixing contributes to the moisture cnvergence in the convective rainfall over the western slopes. However, the boundary layer wind speed contributes in the total rainfall by transporting moisture to the convergent area in the meso-scale flow. Since convective rainfall is the major contributor to the total rainfall, enhancement of desert conditions would decrease surface turbulence mixing resulting in a decrease in the development of the convective activities

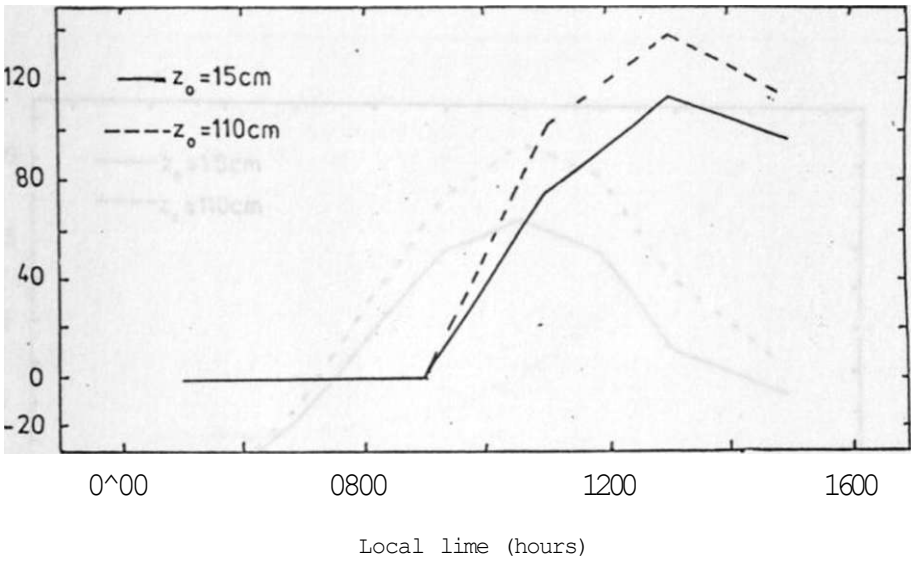

Fig. 38 Temporal variation of lleat flu* from the ground over the Western highlands (Urbanization cose).

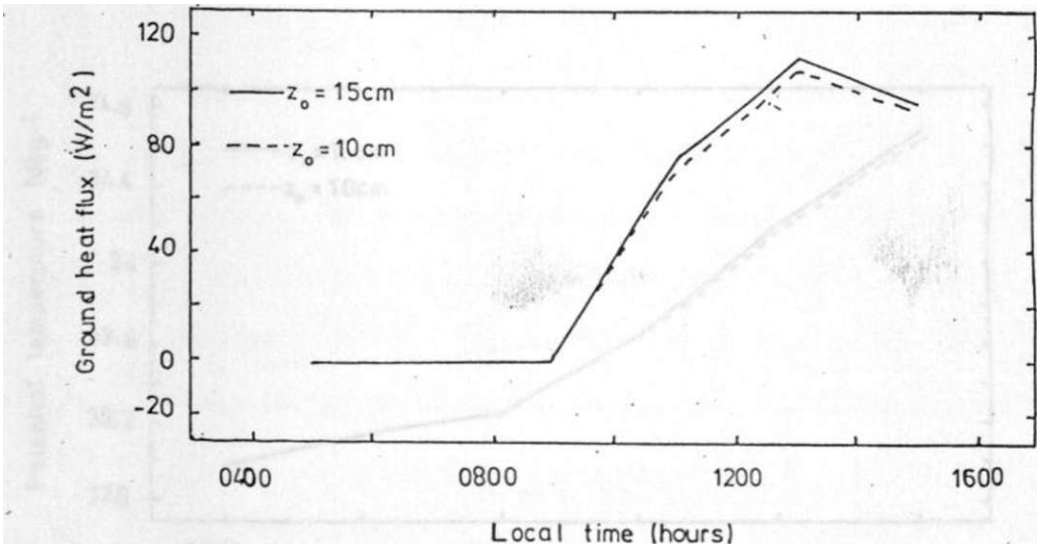

Fig. 39 Temporal Variation of Heat flux from the ground over the Western Highlands (Desertification Case).

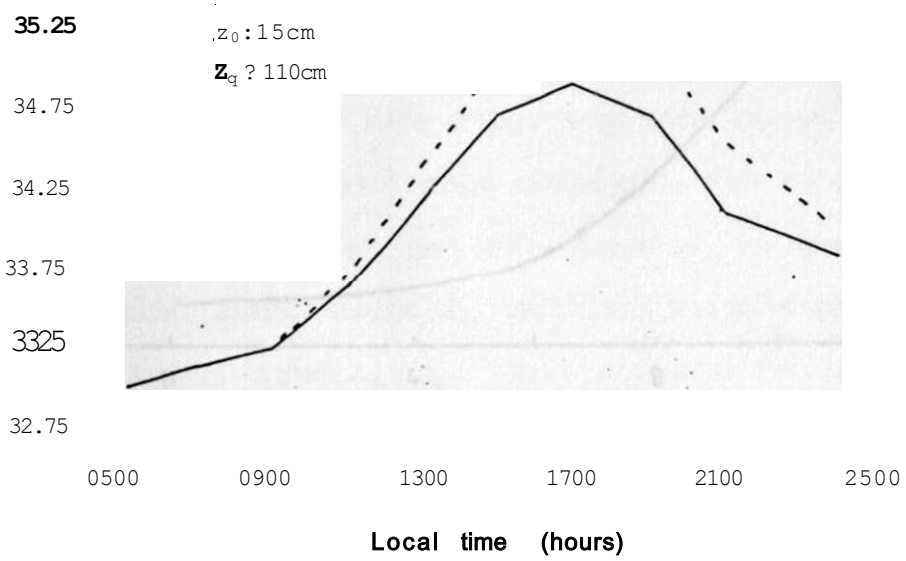

Fig. 40 Temporal Variation of surface layer potential Temperature over the Western Highlands (Urbanization Case).

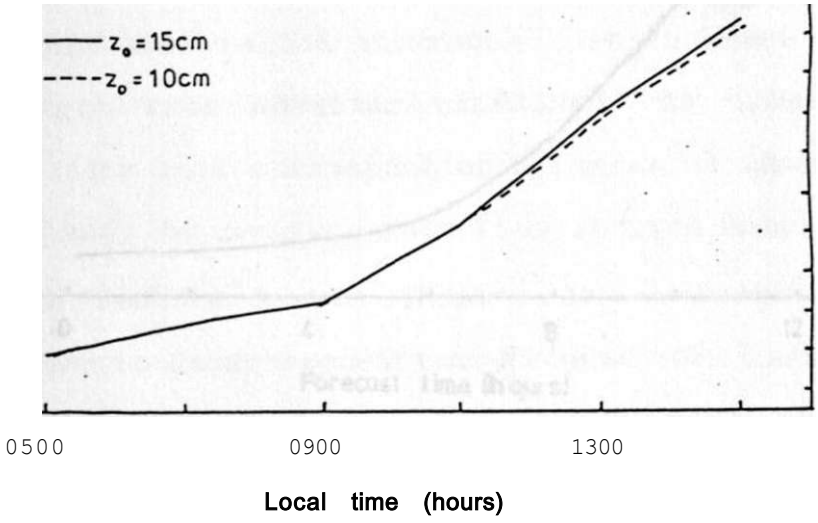

Fig. 41 Temporal Variation of surface layer potential Temperature over the Western Highlands (Desertification Case).

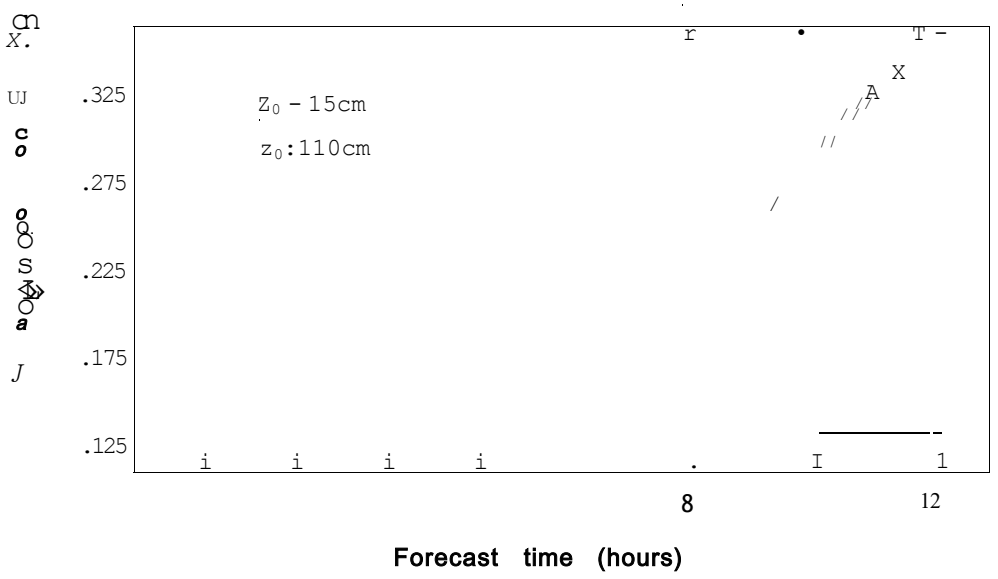

I'ig. 42 Tempornl Variation of Evnporntion from tlie ground over the Western Highlands (Urbanization Case).

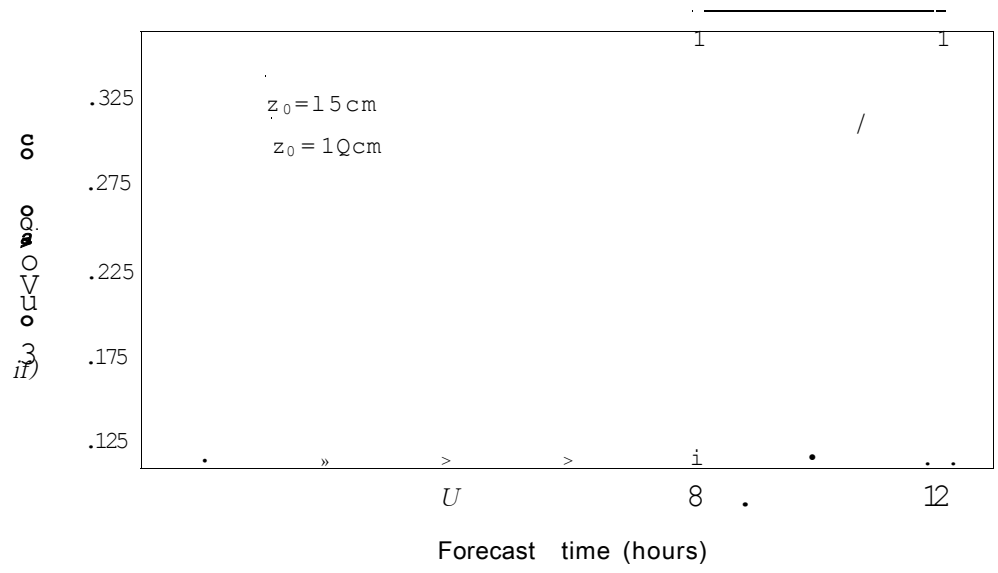

Fig. 43 Tempornl Variation of Evaporation from the ground over the Western Highlands (Desertification Case).

and hence reduction in total rainfall.

3.2.4 HEAT FLUX, SURFACE MOISTURE FLUX AND SURFACE EVAPORATION

In our experiments, only the effect of weather parameters on the surface roughness over Kenya was considered. With all the other terrain features kept constant, the sensible heat flux computed from equation (29) depends on the friction velocity u* and Temperature T*, both of which depend on the surface roughness length, z_Q. An increase in the surface roughness length is expected to give a corresponding increase in sensible heat flux. The temporal variation of ground heat flux over the western highlands (Figures 38 and 39), shows an increase in this parameter with an increase in the surface roughness especially in the afternoon. From the heat budget equation, the sensible heat flux, depends on the solar radiations from the sun. This explains the increase in surface sensible heat in the afternoon. An increase in the roughness length from savannah grasslands to urban area conditions results in a corresponding increase of about 20 Wm^{-2} (about 20%) in sensible heat flux at 1500 hours local time over the western slopes (Figure 38) . Reducing the roughness length to desert conditions (Figure 39), results in a small reduction in sensible heat flux (of about 2%) over the western highlands at 1300 hours local time. An increase in surface roughness results in an increase in turbulent mixing

of heat, causing the increase in the ground heat flux. These results agree with those of Sud et al. (1988), who showed that the heat flux over desert areas was lower than that over areas with a high roughness length. Since, deserts are dry, evaporation is negligible and heat can only be removed from the surface by sensible heat flux and long wave radiative cooling.

Figures 40 and 41 show the temporal variation of surface layer potential temperature over the western slopes. The potential temperature increases with increasing surface roughness length. Increasing the surface roughness to the urban environment would result in an increase of about 0.4°C (about 1.2%) in potential temperature at 1500 hours local time. These results differ from those of Zhang and Anthes (1982), who did a sensitivity study of the surface characteristics and found that increasing the surface roughness resulted in a reduction of the surface layer potential temperature. This decrease in potential temperature was explained to be due to the evaporative cooling in the surface by the increase in the surface evaporation. The difference can be explained to be due to the fact that Zhang and Anthes (1982) used a one dimensional model, which incorporated large scale flow and assumed horizontal advection, and the effect of large rough terrain surfaces to the flow. Pielke (1974) in his study of meso-scale flow over

Florida, showed that increasing the roughness length resulted in increasing the boundary layer potential temperature. Reducing the roughness length through desertification would result in a slight decrease in surface layer potential temperature, as seen in Figure 41.

Surface evaporation is a function of surface characteristics such as albedo, moisture availability, temperature, wind speed, turbulent mixing, etc. In our experiments, the surface characteristics were taken to be homogeneous over the domain of study. Increasing the roughness length to values corresponding to an urban environment (Figures 42 and 43), has no major effect on the surface evaporation over the western highlands. This may be due to the fact that changes in surface roughness length have little effect on surface wind speed. These results however agree with those of Sud et al. (1988) , who found from a general circulation model that changes in the roughness length resulted in little effect on the surface evaporation. Sud et al. (1988), explained this lack of response of surface evaporation to be due to the fact that the experiments were run using the same climatologically prescribed fields of surface albedo and soil wetness. The contribution of surface evaporation to the development of convective activities over the western highlands is negligible as seen from this results.

The results show that varying the surface roughness to

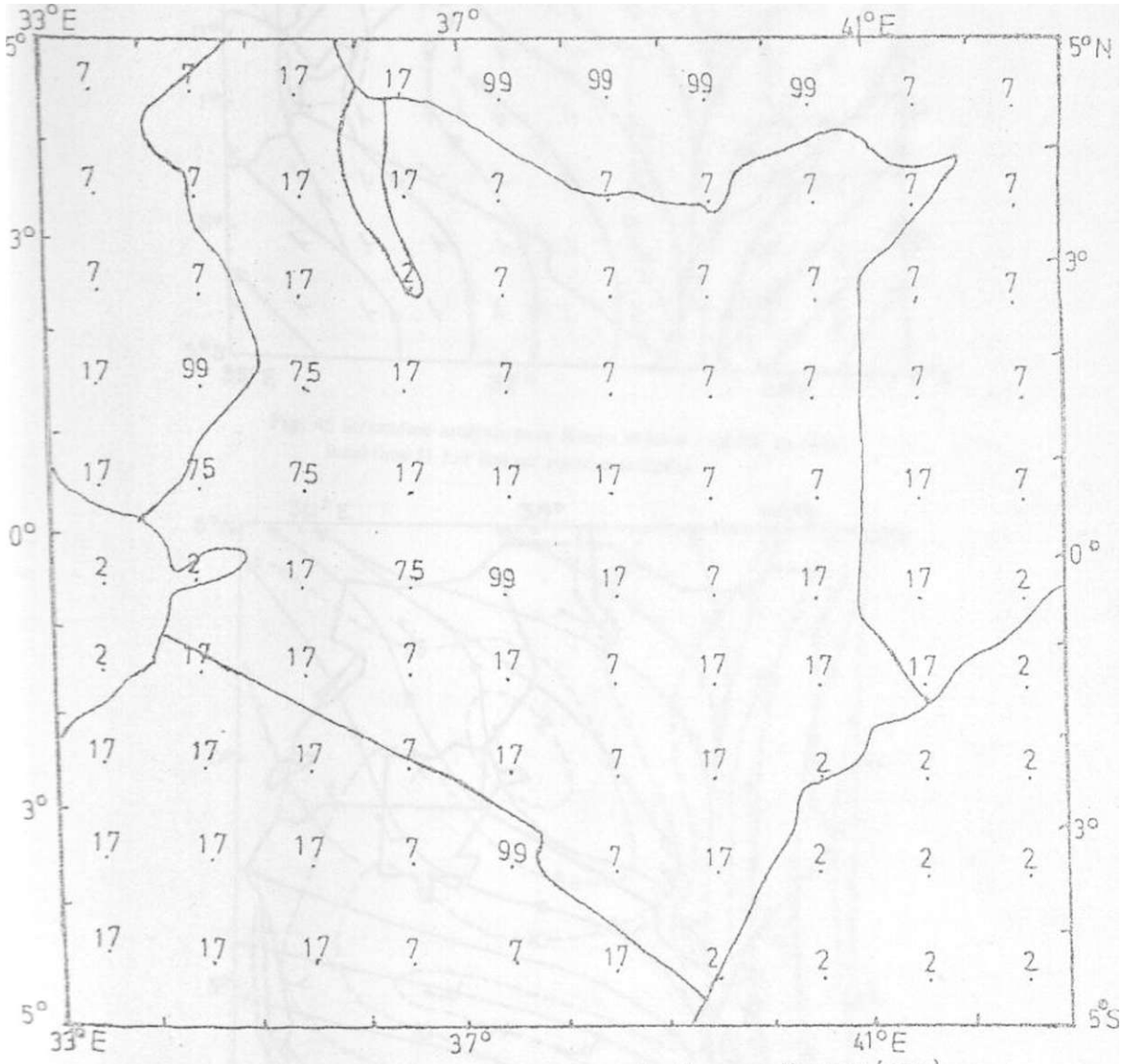

Fig. 44 Grid point specified roughness lenth over Kenya; (cm.)

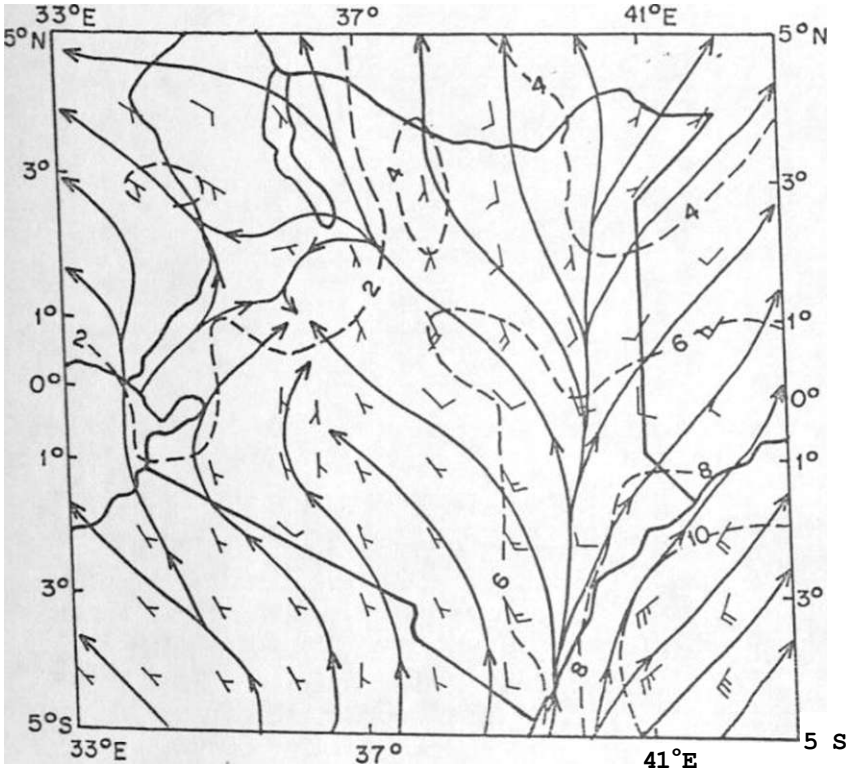

Fig. 45 Streamline analysis over Kenya at level o=0.95, at 1800U local time (1 full feather represents 5m/s)

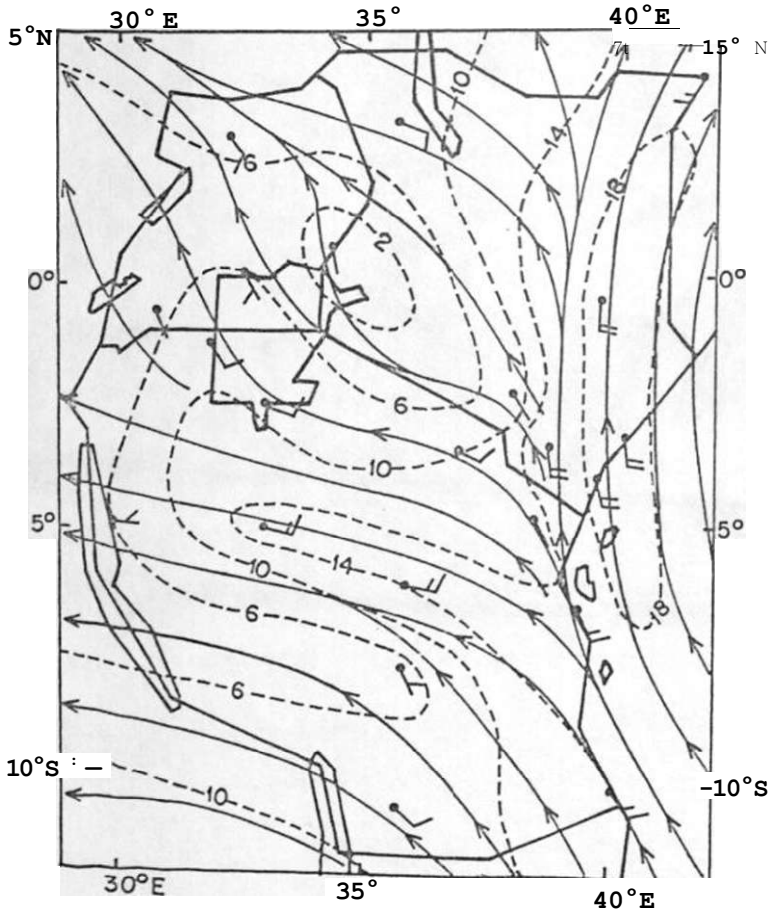

Fig. 46 Mean wind field a, 1525m AMSL in May (Anyamha. 1933)

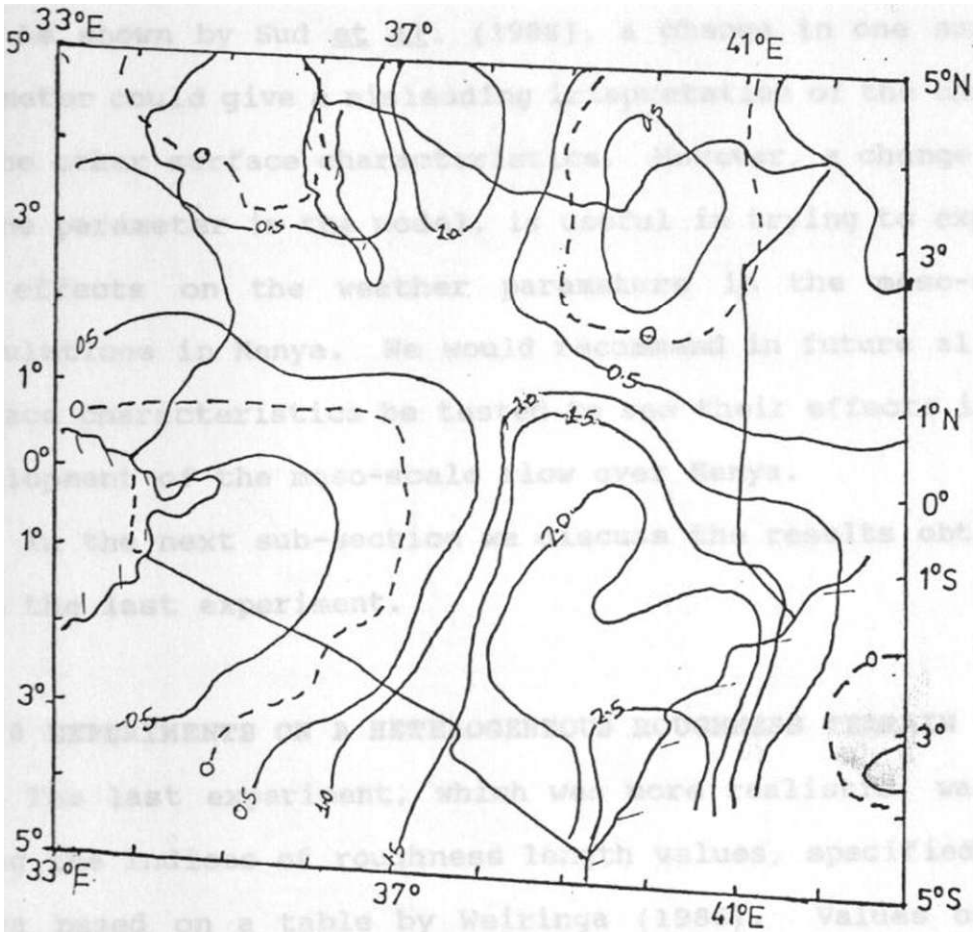

Fie-47 The horizontal divergence field at tr=0.9S, at I800h Local time.

urban conditions or desert conditions, results in the increase or decrease in the surface heat and moisture fields in meso-scale flow over Kenya. The roughness length increases the turbulent mixing resulting in an increase in surface heat flux and moisture flux over the Kenya highlands. However the surface evaporation, does not respond to the changes in the surface roughness.

As shown by Sud et al. (1988) , a change in one surface parameter could give a misleading intepretation of the changes in the other surface characteristics. However, a change just in one parameter in the model, is useful in trying to explain its effects on the weather parameters in the meso-scale circulations in Kenya. We would recommend in future all the surface characteristics be tested to see their effects in the development of the meso-scale flow over Kenya.

In the next sub-section we discuss the results obtained from the last experiment.

3.3.0 EXPERIMENTS ON A HETEROGENEOUS ROUGHNESS TERRAIN

The last experiment, which was more realistic, was run using the indices of roughness length values, specified over Kenya based on a table by Weiringa (1986). Values of the roughness length were specified at each grid point of the domain, based on the physical characteristics of the study area. The types of vegetation cover, geomorphological

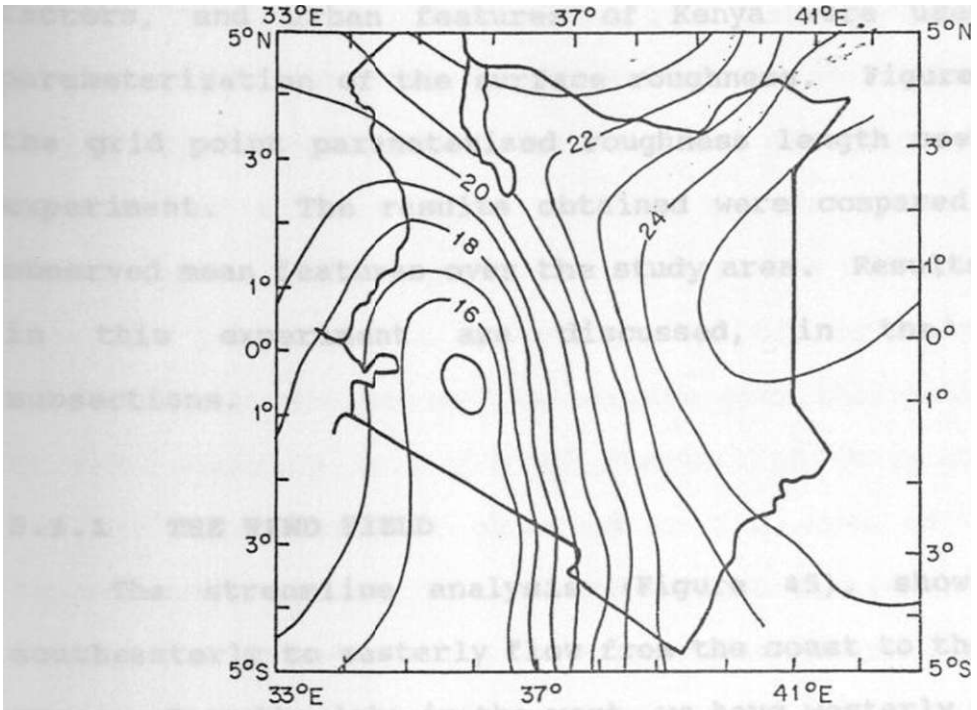

Fig. 48 The temperature field at level σ=0.95 at 1800h local time

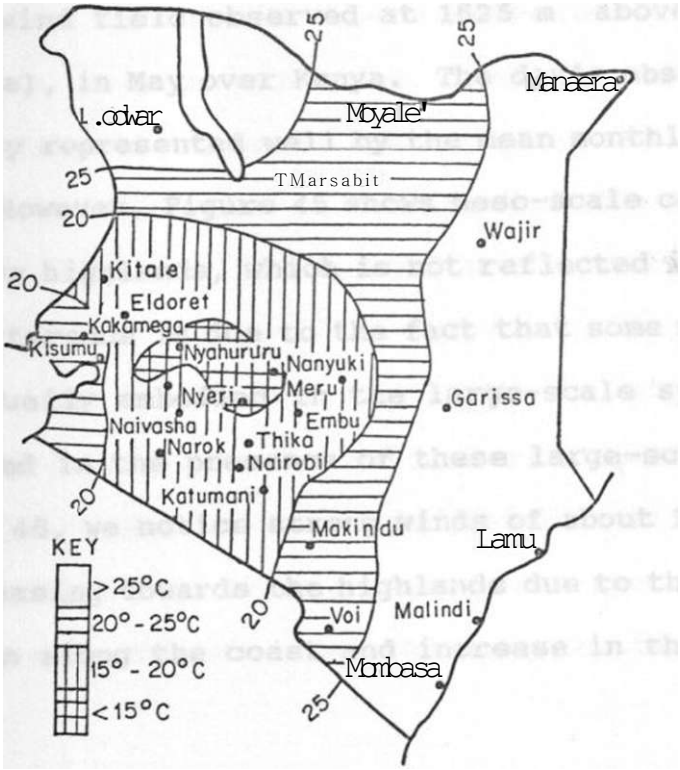

Fig. 49 Air tcmperalurc distribution during May 1936
(Agro-Kenya Met. department)

factors, and urban features of Kenya were used in the parameterization of the surface roughness. Figure 44 shows the grid point parameterized roughness length used in this experiment. The results obtained were compared with the observed mean features over the study area. Results obtained in this experiment are discussed, in the following subsections.

3.3.1 THE WIND FIELD

The streamline analysis (Figure 45), shows general southeasterly to easterly flow from the coast to the highland areas. From the lake in the west, we have westerly flow which converges with the easterlies from the coast over the western highlands. This low-level streamline analysis compares well with the mean wind field observed at 1525 m above mean sea level (a 850 hPa), in May over Kenya. The day's observed wind field is usually represented well by the mean monthly field in the tropics. However, Figure 45 shows meso-scale convergence over the western highlands, which is not reflected in the mean flow. This difference is due to the fact that some meso-scale systems are usually embedded in the large-scale systems and are not observed in the presence of these large-scale flows.

In Figure 45, we notice strong winds of about 11 ms^{-1} from the coast decreasing towards the highlands due to the presence of a jet stream along the coast and increase in the

surface roughness inland. The mean flow pattern for May (Figure 46), shows winds of about 20 knots (a io ms"[1]) over the coast. Over the highly convective areas of western slopes, we observe weak winds of about 1 ms"[1] in the two cases. The line °f streamline diffluence is also seen in the two cases running from the coast to the eastern sector of the country. The confluence in the streamline pattern over the western slopes in the afternoon is a diurnal feature, which is responsible for the active weather observed in this area at this time. However the intensity of convergence is enhanced by the large-scale flow. When the ITCZ is located over Kenya during March-May (long rains) and October-November (short rains) seasons, the meridional component of the ITCZ induces some incursions of moist westerly winds from the moist Congo/Zaire basin and Atlantic ocean, which enhance the meso-scale lake breeze. Similarly, the region experiences strong southeasterly monsoons from the coast towards the highlands at this time. The convergence between the easterlies and the westerlies determines the intensity and location of the meso-scale convergence.

The horizontal divergence field (Figure 47), shows a **marked** low-level divergence over the eastern slopes, with low-level convergence observed over the western slopes. The convergence observed over the northeastern areas of Kenya is less important since these areas are generally dry.

conclusion, the simulated flow patterns on a -terogeneous terrain over Kenya, compare well with the mean -cse^rvec3 wind flow patterns.

3.3.2 THE TEMPERATURE FIELD

The low-level temperature field over Kenya is shown in r^^ur-e 48. The figure shows high temperatures of over 25°C oveir "the eastern highlands. The temperature decreases towards highlands to about 15°C. High temperatures are again stained over the arid/semi arid parts and the lake region as -s usually observed. This temperature field compares well with. the observed mean values for May 1986 (Figure 49) .

The low-level temperature field is important in creating **the pressure** gradient between land and water so as to generate the **meso**-scale circulations. Apart from the dependence of the **temperature** pattern over Kenya on solar heating, the complex **terrain** and turbulent mixing of heat by the surface roughness **also** contribute to it.

The results show that the boundary layer temperature **field** simulated on a heterogeneous terrain over Kenya compare well with the observed mean values.

3.3.3 HUMIDITY, VERTICAL MOTION AND RAINFALL

The low-level humidity field over Kenya (Figure 50), show values of up to 99% over the western slopes of highlands.

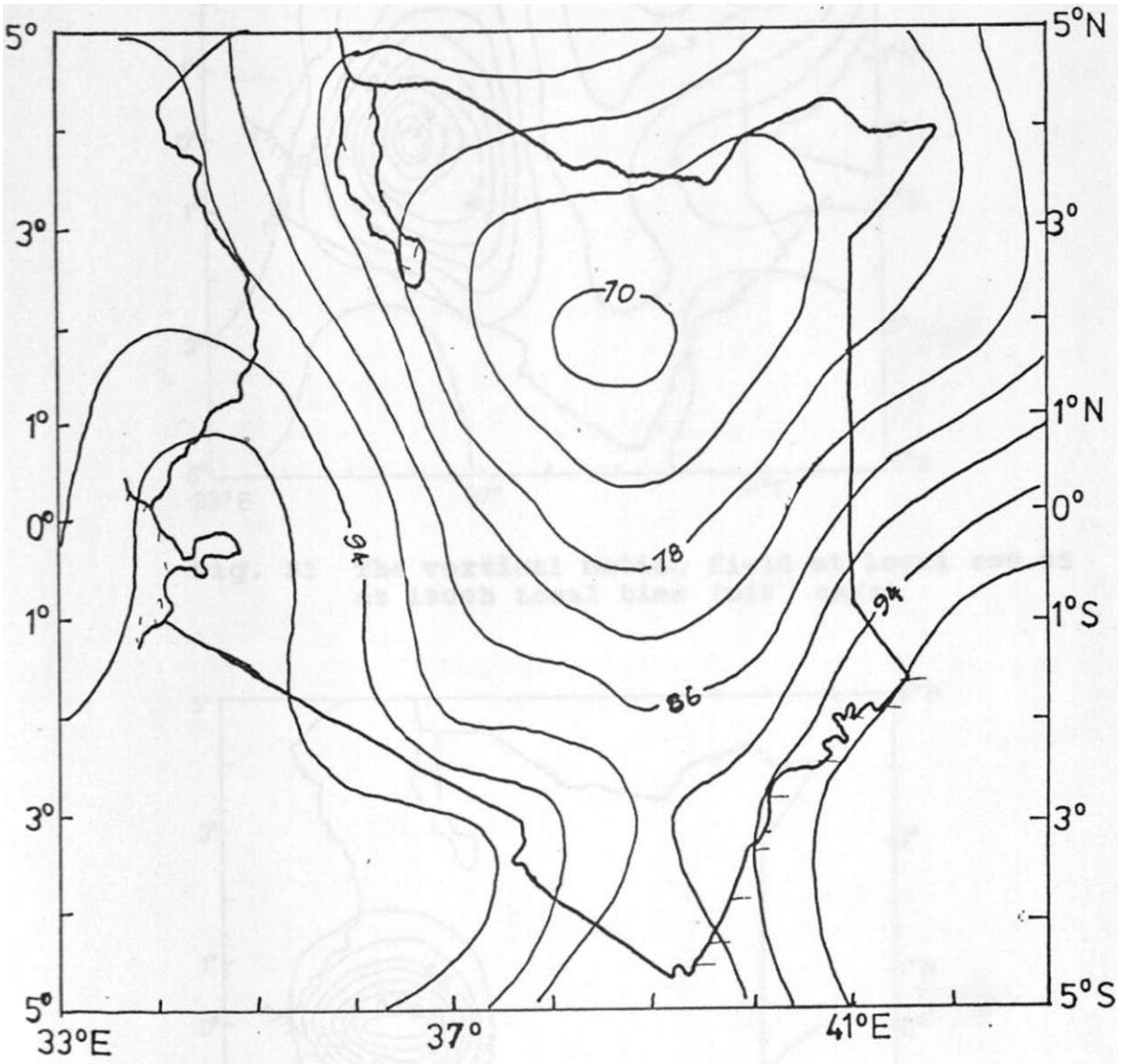

Fig. 50 The relative humidity field at level <T=0.95 at 1800 Local time.

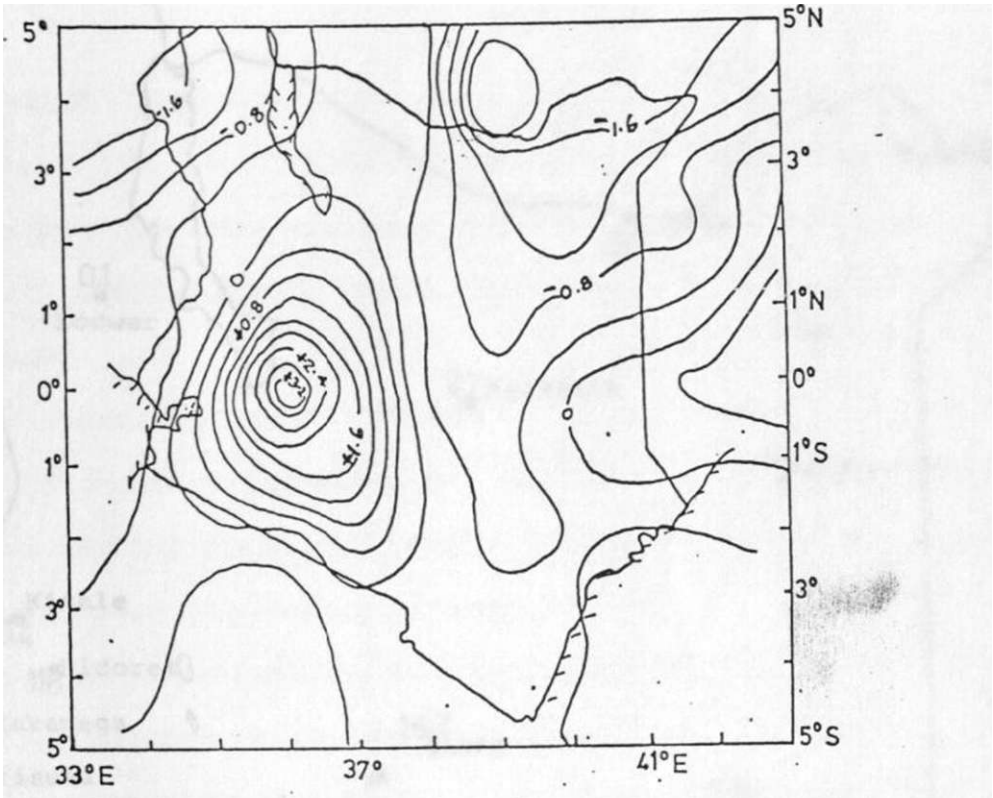

Fig. 51 The vertical motion field at level σ=0.95 at 1800h Local time (x10^{-1} cm/s)

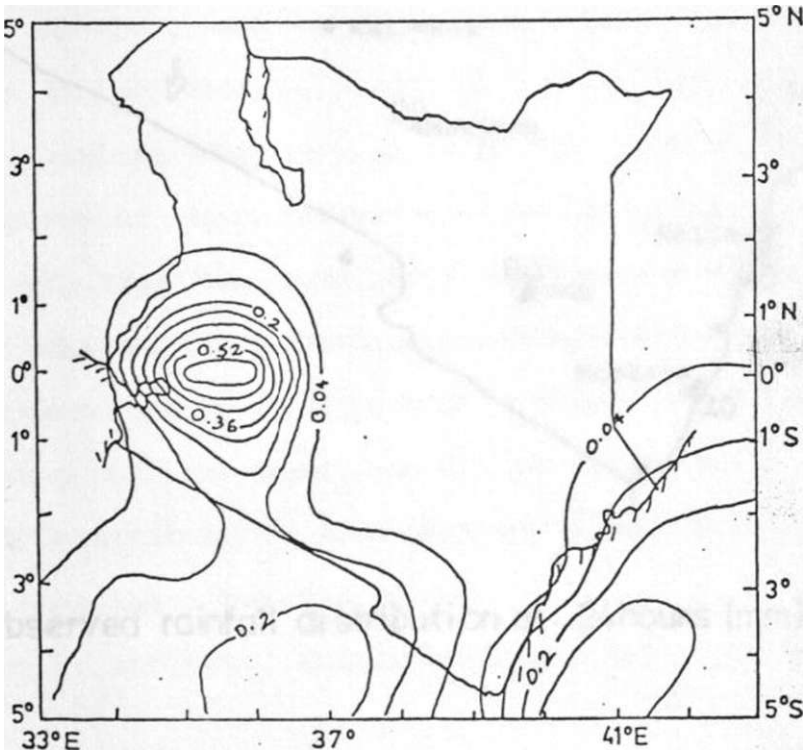

Fig. 5X Accumulated Total Rainfall at 1800h Local time (mm)

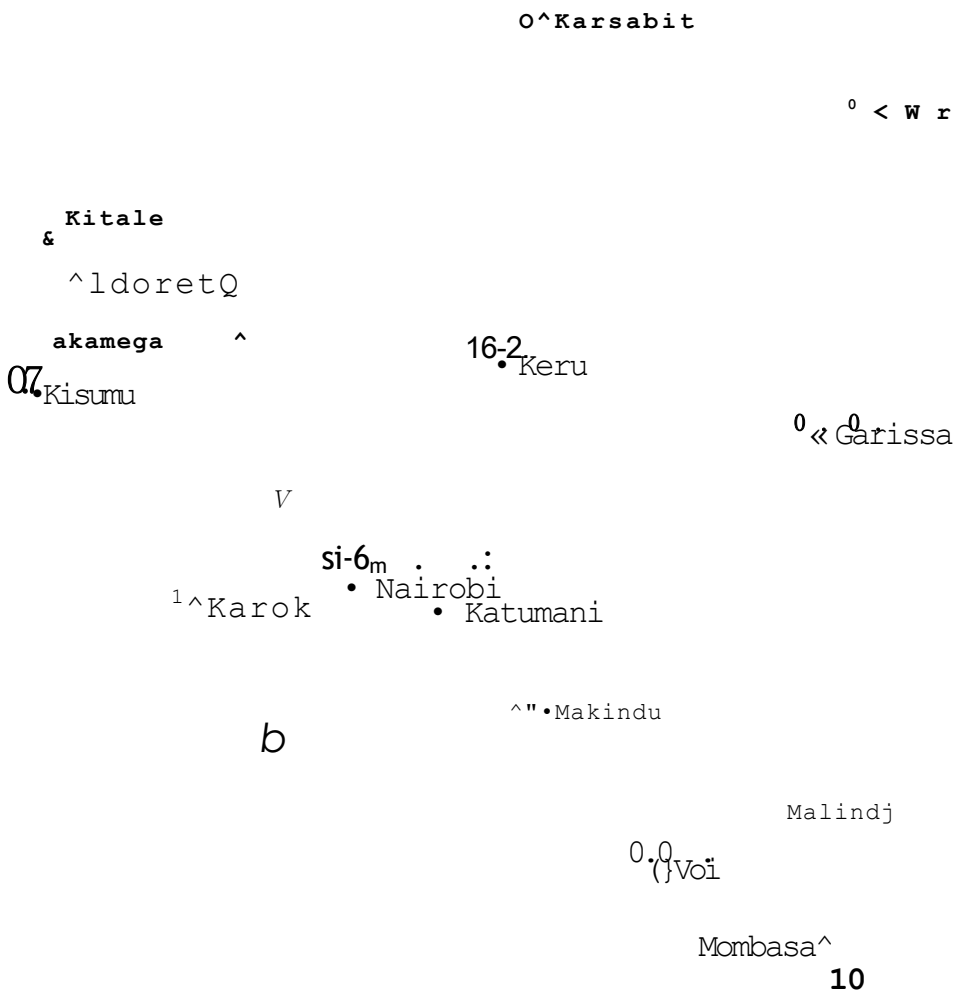

Fig.53 Observed rainfall distribution at 2£hours (mm)

High values are simulated over the water bodies of lake victoria to the west and indian ocean to the east. Areas with minimum moisture were concentrated over the arid and semi-arid parts of northeastern Kenya where values below 70% were indicated.

The accumulation of moisture over the western slopes is responsible for triggering the convective rainfall usually observed in this areas in the afternoon. The turbulent mixing as a result of the surface roughness has been shown by this study to be one of the major determinants of the amount of moisture convergence in the meso-scale flow over Kenya. The model however simulates high values than is usually observed. This could be resulting from the model formulation of the moisture field.

The vertical motion field (Figure 51), shows rising motion in the convective areas of the western slopes of the highlands and sinking motion over the east facing slopes. Rising motion of about 3.0x10"' cms"[1] is simulated at the second sigma level from the ground (- 820 hPa) over the western slopes. The vertical motion is enhanced by the low-level moisture convergence in this area during the afternoon hours. The sinking motions over the dry eastern parts of central highlands contribute to the observed clear skies over these areas during the afternoon hours.

Most of the total accumulated rainfall over the western

slopes as shown in Figure 52, is generated from the convective rainfall. Turbulent mixing as a result of heterogeneous surface roughness, contributes to this convective rainfall as seen earlier. Total accumulated rainfall of about 0.72 mm is simulated at 1800 hours local time. Along the coast, the model simulates relatively less accumulated rainfall. These coastal areas benefit from the advected moisture from the Indian ocean. No rainfall was simulated over the dry parts of eastern and northern Kenya.

The observed 24-hour rainfall totals for May 6 1986 (Figure 53), shows the concentration of the peak rainfall values over the western slopes, in close agreement with the model simulations. No raifall was observed over the eastern slopes. Some spatial differences were however quite evident. The differences in the simulated and observed rainfall intensity may be partly explained in terms of the contributions by large-scale systems which are not considered in the meso-scale experiments.

The results obtained in this study compare well with the observed conditions for May 6 1986 over Kenya. We would however expect proper specification of the other surface parameters such as albedo, moisture availability, thermal capacity, etc., to give better simulations of meso-scale flow over Kenya. These results however, form a basis for any future applications of the effects of the roughness length

over the region. The surface roughness indices used in this study was representative of the region, and can be modified accordingly with the changes in the physical characteristics of the underlying local surfaces before being used in the meso-scale numerical experiments over Kenya. In future it will be of interest to perform enough observations of turbulent statistics over Kenya. This will lead to establishing an effective roughness for use in numerical study of meso-scale flow over Kenya.

In the next chapter conclusions and suggestions for further extension of this study are given.

CHAPTER 4

4.1.0 SUMMARY AND CONCLUSIONS

The main objective of this study was to investigate the effects of changing roughness length on the meso-scale flows over Kenya, using a numerical model. The model used was a three-dimensional meso-scale model developed by Anthes and Warner (1978). This model has been adapted to the geography of the region by Okeyo (1987).

Three numerical experiments were conducted. The first experiment attempted to examine the ability of the model to simulate meso-scale systems. The last two experiments involved the use of the roughness length based on homogeneous and heterogeneous terrains, respectively.

In order to simulate the meso-scale flow over Kenya, the wind field was initialized to zero at 0500 hrs local time. The results from the first experiment indicated that the model was capable of giving realistic diurnal cycles of the meso-scale circulations. The simulated diurnal characteristics (both horizontal and vertical patterns of the land/sea and mountain/valley winds) were in close agreement with the observed characteristics. In the afternoon, upslope flow coupled with the lake breeze from lake Victoria developed over the western sector of the domain while the sea breeze from the Indian ocean was observed over the eastern sector. The most

extensive cloud formation took place at around 1800 hours local time, especially over the western slopes. This corresponds to the time of maximum vertical motion and convective developments.

The results from the simulations with a homogeneous roughness terrain showed a reduction in the boundary layer wind speed as the surface roughness was increased. The transfer of heat and moisture by turbulent mixing in the meso-scale convergent areas however increased as the surface roughness was increased. The temporal variations of the potential temperature in the surface layer, the specific humidity and convective rainfall also increased over the western slopes with the increase in the roughness length. This increase was explained in terms of the increase in turbulent mixing of heat and moisture in the meso-scale convergent areas. The non-convective rainfall was however reduced when the surface roughness increased. This is due to the reduction in the advection of moisture and heat. The reduction in the non-convective rainfall was however not marked, as the total simulated rainfall was mainly convective.

In the last experiment, involving the use of a heterogeneous roughness terrain, the simulated wind speeds were stronger in the eastern parts of the domain and decreased towards the highlands. This could be due to the changes in the surface roughness. Streamline analysis showed convergence

over the western slopes. Low-level divergence was dominant over the eastern slopes and the coast. The temperature field showed high values over the coastal areas and lake basin with low values centered over the highlands. The boundary layer moisture convergence over the western slopes was enhanced by the turbulent mixing to give the observed afternoon active weather in this region.

The results from this study are important in the development of numerical weather prediction models for Kenya. They can also be used in the planning and management of human activities which affect meso-scale climates.

Suggestions on the extension of this work are discussed in the following subsection.

4.2.0 SUGGESTED FURTHER STUDIES

In this study we have shown that the meso-scale flow pattern over Kenya is sensitive to the surface roughness length. There are however other surface characteristics (i.e. albedo, soil wetness, thermal capacity, etc.) which need to be tested in order to determine the contributions of the other processes to the development of meso-scale flows over Kenya. This will lead to better parameterization of surface characteristics in order to improve the meso-scale models over the region. We therefore recommend that sensitivity tests be done on the other surface parameters to determine their

contribution in the development of meso-scale flows.

In order to avoid the grid point specification of the roughness length over Kenya, appropriate observations must be made to find an "effective" roughness for use over the region as defined by Fiedler and Panofsky (1972).

The model should be extended to cover other East and Central parts of Africa, and to incorporate large-scale flows. Proper initialization should be made so as to allow the study of individual seasons of the year i.e. Northern hemisphere Summer, Winter, Autumn and Spring independently. This improvement will enable the model give more realistic forecasts of the regional weather.

ACKNOWLEDGEMENTS

The author is indebted to the supervisors, Prof. Ogallo and Dr. Anyamba of the University of Nairobi for their consistent guidance and encouragement during the research period, and their conscientious review of the research and various manuscripts which led to this final volume. The appreciation also goes to the University of Nairobi through the Chairman of the Department of Meteorology for availing me the scholarship to pursue this course. I also thank the Director of Kenya Meteorological Services for releasing me to pursue the course, and all the staff of the Drought Monitoring Center, Nairobi, for their help in computer work.

My final thanks go to my mother Selinah Chevuneko, father Reuben Indeje and all the family members for their patience and moral support.

The list of those to be thanked is of course too long to be compiled here, but it is hoped that my message of acknowledgement will reach those of you who will have a chance to read this volume.

REFERENCES

Alusa, A.L; 1976: The occurrence and nature of hailstorms in Kericho, Kenya. *Proc. 2nd sci. conf. on weather mod. Boulder, Colorado-IAMAP/WMO,* pp. 249-256.

Andre, J. C. and C. Blondin; 1986: On the effective roughness for use in numerical three-dimensional models. *Bound, lay. Meteor; 35,* 231 - 245.

Anthes, R.A; 1977: A cumulus parameterization scheme using one-dimensional cloud model. *Mon. Wea. Rev; 105,* 270-286.

, and E.Y. Kuo; 1987: Description of the penn state/NCAR meso-scale model version 4 (MM4). *Acid Deposition modelling project Boulder, Colorado.*

, and T.T. Warner; 1978: The development of meso-scale models suitable for air pollution and other **meso**-meteorological studies. *Mon. Wea. Rev; 106.* 1045-1078.

Anyamba, E. K; 1983: On the monthly mean lower troposphere circulation and anomalous circulation during the 1961/62 floods in East Africa. *M.sc Thesis, Dept. of Met. University of Nairobi.*

Asnani, G.C. and J.H. Kinuthia; 1979: Diurnal variation of precipitation in East Africa. *Kenya Met. Dept. Research Report No. 8/79,* 1-58.

Deardorff, J.W; 1978: Efficient prediction of ground surface temperature and moisture with inclusion of a layer of vegetation. *J. Geophys. Res; 83,* 1889-1903.

Fiedler, F. and H.A. Panofsky; 1972: The geostrophic drag coefficient and the effective roughness length. *Quart. J. Roy. Meteor. Soc; 98,* 213-220.

Findlater, J; 1971: Mean monthly airflow at low-levels over the western Indian ocean. *Geophys. memo. No. 115,* HMSC. Lond. UK.

Garrat, J.R; 1977: Aerodynamic roughness and mean monthly surface stress over Australia. *C.I.R.O Aust. Div. Atmos. Phys. Tech. Paper No. 29,* 1-19.

Hansen, J., G. Russel, D. Rind, P. Stone, A. Lacis, S. Lebedeff, and L. Travis; 1983: Efficient three-dimensional global models for climate studies. Models I and II. *Mon. Weath. Rev; 111,* 609-662.

Hsie, E.-Y. and R.A. Anthes; 1984: Simulation of frontogenesis in a moist atmosphere using alternative parameterizations of condensation and precipitation. *J. Atmos. Sci; 41,* 2701-2716.

Johnson, D.H., and H.T. Morth; 1960: Forecasting research in East Africa. *Proc. of Symposium on trop. met. in Africa. Munitalp foundation, Nairobi, Kenya, 56,* 137pp.

Kuo, H.L; 1974: Further studies of the parameterization of the influence of cumulus convection on large-scale flow. J. *Atmos. Sci; 31,* 1232-1240.

, and R.A. Anthes; 1984a: Accuracy of diagnostic heat and moisture budgets using SESAME-79 field data as revealed by observing system simulation experiments. *Mon. Wea. Rev; 102,* 1465-1481.

Lumb, F.E; 1970: Topographic influences in the thunderstorm activity near Lake Victoria. *Weather, 25,* 404-414.

Mahrer, Y. and R.A. Pielke, 1977: Effects of topography on land and sea-breezes in a two-dimensional model. *Mon. Wea. Rev; 105,* 1151-1162.

Majugu, A.W; 1983: Mean and seasonal diurnal variation of precipitation in East Africa. *M.SC. Thesis Dept. of Met. University of Nairobi.*

National Atlas of Kenya. Third edition 1970.

Njau, L.N; 1982: Tropospheric wave disturbance in East Africa. *M.SC. Thesis Department of Met, University of Nairobi.*

Ogallo, L.A.J; 1984: Climatology of rainfall in East Africa. *WMO Trop. Met. Prog. Scientific conference on GATE, WAMEX and Tropical Met. in Africa,* Dakar, 10-14 Dec. 1984.

Okeyo, A. E; 1982: A two-dimensional model of the land-lake and sea-land breezes over Kenya. M.SC. *Thesis, University of Nairobi.*

, 1987: Towards the development of a forecasting numerical model for Kenya. *PHD. Dissertation Department of Meteorology, University of Nairobi.*

Ojany, F.F. and R.B. Ogendo; 1988: Kenya. A study in physical and human geography. *Longman Kenya Limited, Nairobi;* 2 55pp.

Perkey, D.J., and C.W. Kreitzberg; 197 6: A time dependent lateral boundary scheme for limited-area primitive equation models. *Mon. Wea. Rev; 104,* 744-755

Pielke, R.A; 1974: A three-dimensional model of the sea-breeze over South Florida. *Mon. Wea. Rev; 102,* 115-139.

Rowntree, P.R; 1983: Simulation of the atmospheric response to soil moisture anomalies in Europe. *Quart. J. Roy. Met. Soc; 109,* 501-526.

, 1988: Land surface parameterization - Basic concept and review of the schemes. *ECMWF Workshop Proc, Shinfield Park, Reading U.K;* 24-26 oct. 1988.

the ITCZ.

1963. The structure and behavxor of

Sanson, H.W; ^ t nd pesert

Proc. Of *the mo,TAG* seminar *on*

locusts. Tehran, 25 Nov -11 Dec

and s.N. Gichuiya; 1971: **Hailstorms** in Kericho.

EAMD Tech. memo. No. 22, 6pp.

Sellers, P.J* V. Mintz, Y.C. Sud, and A. Dalcher; 1936:

A simple biospheric model for use within GCM.

j. *atmos. sci; 43,* 505-531.

; E.R. **Albertazzi,** J.L. Dorman, Y.T. Hou, J.L.

Kinter, D.A. Randall, N. Sato, E.K. Scheneidor,

Shukla, and W.J. Shuttleworth ; 1988: Model ling

land surface processes at the centre for

ocean-land-atmosphere interactions (Col.i),

University of Maryland. *EMCWF Seminar,* 9-1 » r.ept .

1988.

Smith, F.B, and D.J. Carson; 1977: Some thoughts on the

specification of boundary layer relevant to

numerical modelling. *Bound, layer. Met; 12,* \oi-\

Sud, Y.C., and **W**.e. Smith; 1985a: The influence of

surface roughness of desert on July **circulation.** (A

numerical study). *Bound, layer. Meteor; 33.*

, and M.J. Fennessy; **1985b:**

influence of local land surface processes on

the Indian monsoon. A numerical study. Journ

Climate and *Applied* Het. 24/ m5_1036_

, J. Shukla and Y. Mintz; 1988: Influence of surface roughness on atmospheric circulation and precipitation. A sensitivity study with general circulation model. *Journ. of Appl. Met; 27,* 1036-1054.

Tomsett, J.E; 1969: Average monthly and annual rainfall maps of East Africa. *EAMD Tech. Memo; No. 14.*

Thompson, B.W; 1957: Some reflections on equatorial and tropical forecasting. *EAMD Tech. memo; No. 3,* 219-220.

Warner, T.T., R.A. Anthes, and A.L. McNab; 1978: Numerical simulations with a three-dimensional meso-scale model. *Mon. Wea. Rev; 106,* 1079-1099.

Weiringa, J; 1986: Roughness-dependent geographical interpolation of surface wind-speed averages. *Quart. J. Roy. Meteor. Soc; 112,* 867-889.

WMO; 1970: Urban climates. *Technical Note No. 108,* 390pp.

Yanai, M., S. Esbenson, and J. Chu; 1973: Determination of bulk properties of tropical cloud clusters from the large-scale heat and moisture budgets. *J. Atmos. Sci; 30,* 611-627.

Zhang, D. and R.A. Anthes; 1982: A high-resolution model of the planetary boundary layer-Sensitivity tests and comparison with SESAME-79 data. *Jour, of Appl. Meteor; 21,* 1594-1609.